First-principles quantum transport modeling of thermoelectricity in nanowires and single-molecule nanojunctions

Branislav K. Nikolić

Department of Physics and Astronomy, University of Delaware, Newark, DE 19716, U.S.A.

http://wiki.physics.udel.edu/qttg

References

J Comput Electron (2012) 11:78–92
DOI 10.1007/s10825-012-0386-y

First-principles quantum transport modeling of thermoelectricity in single-molecule nanojunctions with graphene nanoribbon electrodes

Branislav K. Nikolić · Kamal K. Saha · Troels Markussen · Kristian S. Thygesen

RAPID COMMUNICATIONS

PHYSICAL REVIEW B **84**, 041412(R) (2011)

Multiterminal single-molecule–graphene-nanoribbon junctions with the thermoelectric figure of merit optimized via evanescent mode transport and gate voltage

Kamal K. Saha,[1] Troels Markussen,[2] Kristian S. Thygesen,[2] and Branislav K. Nikolić[1,*]
[1]*Department of Physics and Astronomy, University of Delaware, Newark, Delaware 19716-2570, USA*
[2]*Center for Atomic-scale Materials Design (CAMD), Department of Physics, Technical University of Denmark, DK-2800 Kongens Lyngby, Denmark*

http://arxiv.org/abs/1201.1665

Edge currents and nanopore arrays in zigzag and chiral graphene nanoribbons as a route toward high-*ZT* thermoelectrics

Po-Hao Chang and Branislav K. Nikolić
Department of Physics and Astronomy, University of Delaware, Newark, DE 19716-2570, USA

PHYSICAL REVIEW B **81**, 155450 (2010)

Electron density and transport in top-gated graphene nanoribbon devices: First-principles Green function algorithms for systems containing a large number of atoms

Denis A. Areshkin and Branislav K. Nikolić
Department of Physics and Astronomy, University of Delaware, Newark, Delaware 19716-2570, USA

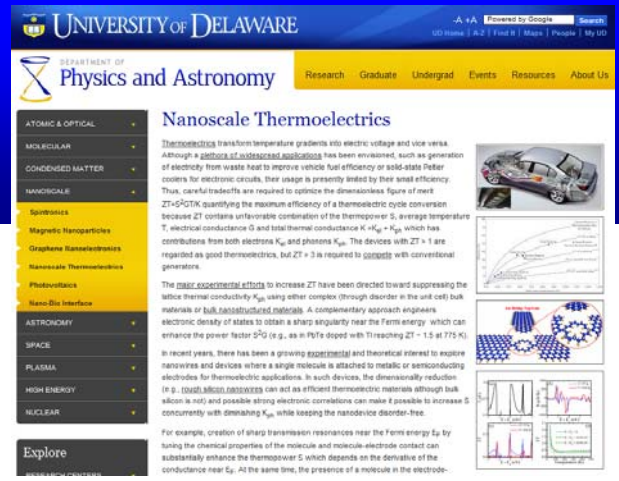

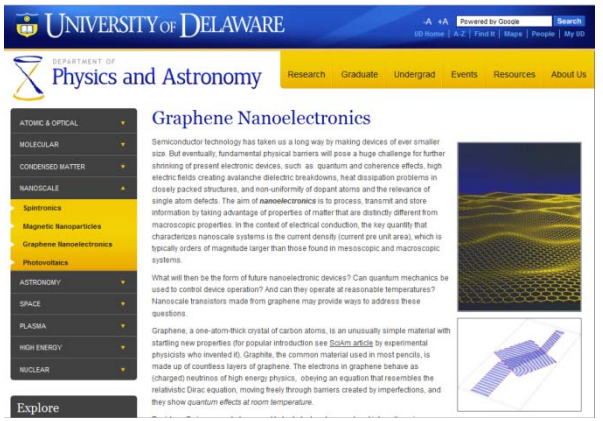

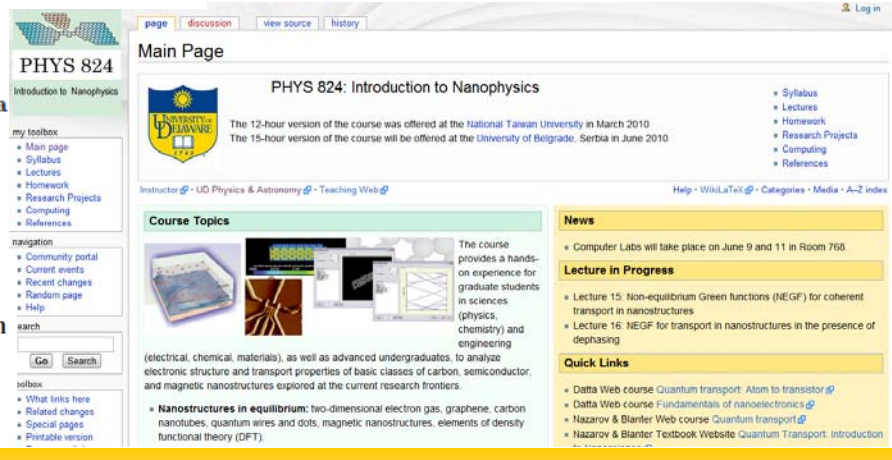

Thermoelectric Phenomena: Fundamentals and Applications

Fundamentals

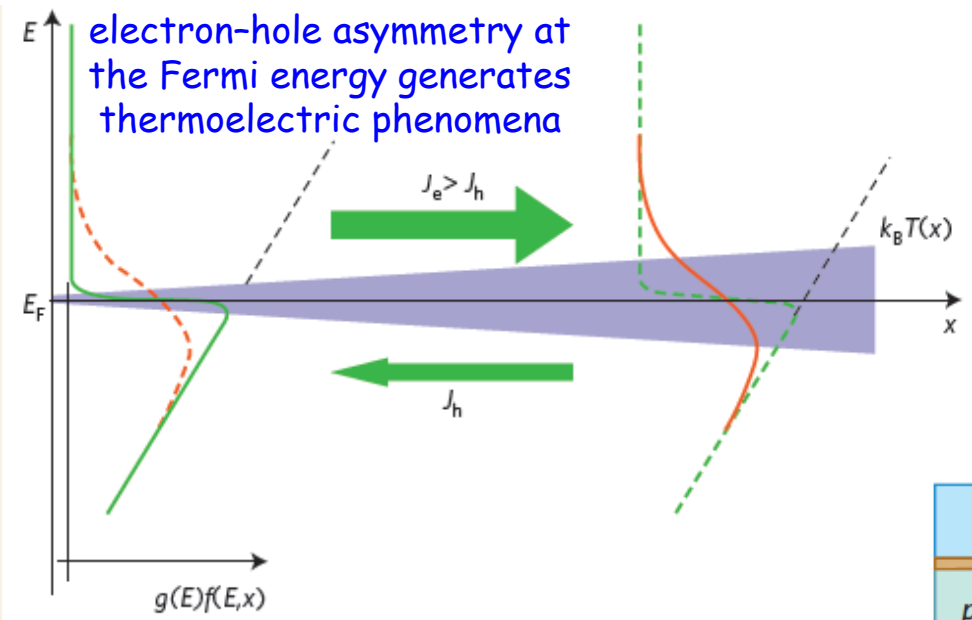

bulk

$$\begin{pmatrix} \mathbf{E} \\ \mathbf{Q} \end{pmatrix} = \begin{pmatrix} 1/\sigma & S \\ \Pi & K \end{pmatrix} \begin{pmatrix} J \\ -\nabla T \end{pmatrix}$$

constrictions and interfaces

$$\begin{pmatrix} -\Delta V \\ \mathbf{Q} \end{pmatrix} = \begin{pmatrix} 1/G & S \\ \Pi & \kappa \end{pmatrix} \begin{pmatrix} I \\ -\Delta T \end{pmatrix}$$

$$K = K_{\mathrm{el}} + K_{\mathrm{ph}}$$

$$\kappa = \kappa_{\mathrm{el}} + \kappa_{\mathrm{ph}}$$

Applications

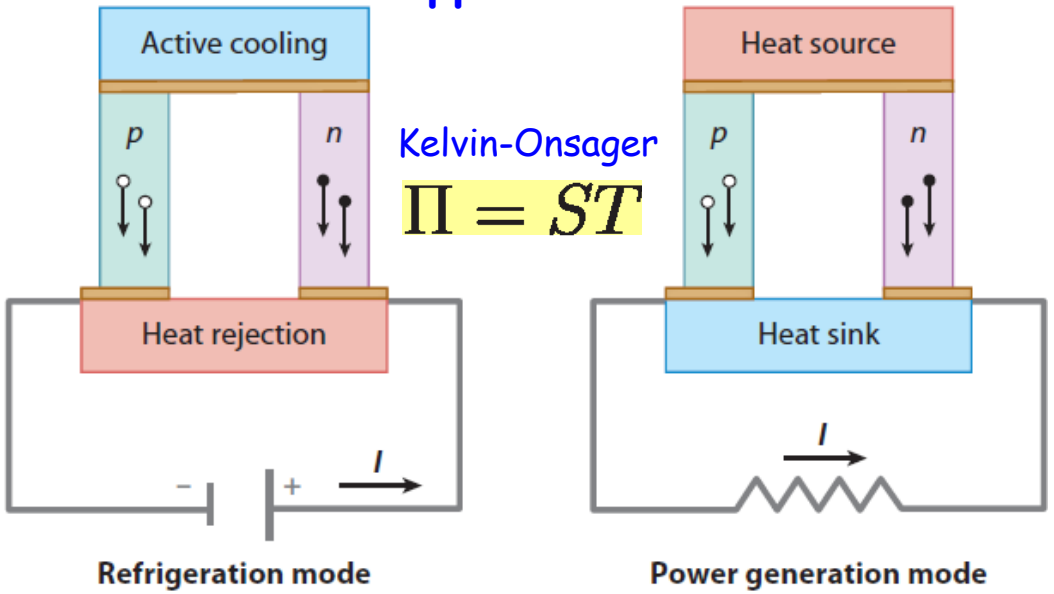

Thermoelectric Figure(s) of Merit ZT in the Linear-Response Regime

$$ZT = \frac{S^2 G T}{\kappa_{\rm el} + \kappa_{\rm ph}}$$

$$ZT = \frac{(S_p - S_n)^2 T}{[(\kappa_n/\sigma_n)^{1/2} + (\kappa_p/\sigma_p)^{1/2}]^2}$$

- In the linear-response regime (i.e., close to equilibrium) one operates close to the small voltage V = - S ΔT which exactly cancels the current induced by the small temperature bias ΔT
- As ZT → ∞, the efficiency approaches the ideal Carnot value

$\eta_C = 1 - T/(T+\Delta T)$

- thus, in the linear-response regime ΔT « T typically investigated for bulk materials, the efficiency stays low $\eta_C = \Delta T / T$ even if ZT can be made very large

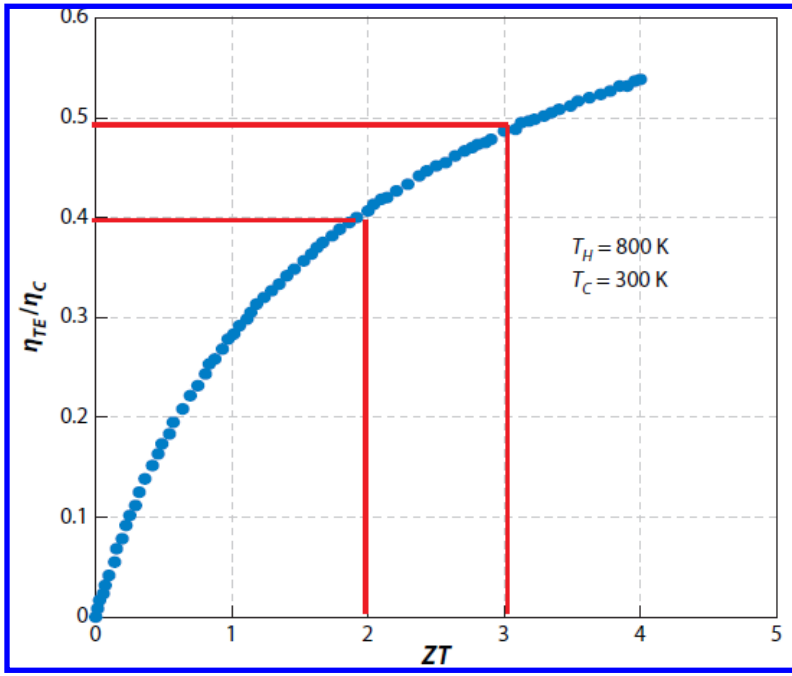

$$\eta_{\rm TE} = \frac{W}{Q_H} = \frac{T_H - T_C}{T_H}\left(\frac{(1+ZT_M)^{1/2} - 1}{(1+ZT_M)^{1/2} + T_C/T_H}\right)$$

Ultimate pragmatic goal:
devices with $ZT \approx 2$–3 that are stable over a broad temperature range with low parasitic losses

Decades of Little Progress in Increasing ZT of Bulk Materials

An inconvenient truth about thermoelectrics

Nature Mater. **8**, 83 (2009)

Cronin B. Vining

Despite recent advances, thermoelectric energy conversion will never be as efficient as steam engines. That means thermoelectrics will remain limited to applications served poorly or not at all by existing technology. Bad news for thermoelectricians, but the climate crisis requires that we face bad news head on.

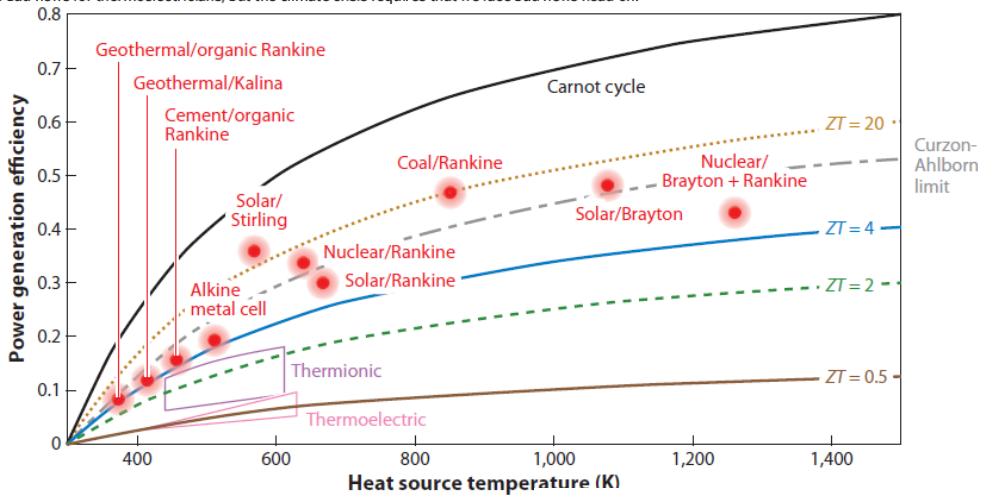

"phonon glass-electron crystal"

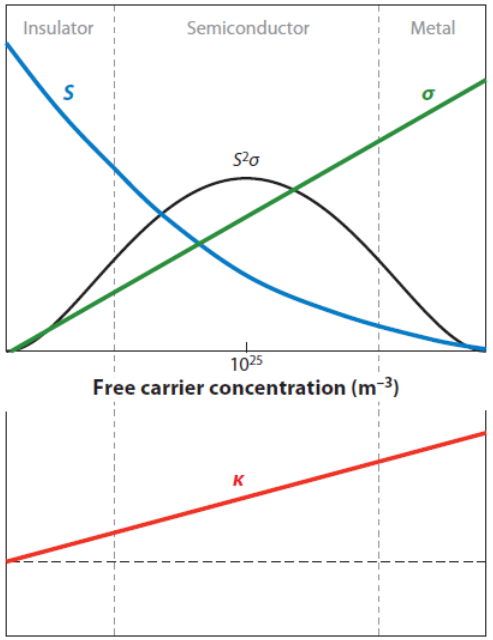

complex bulk materials

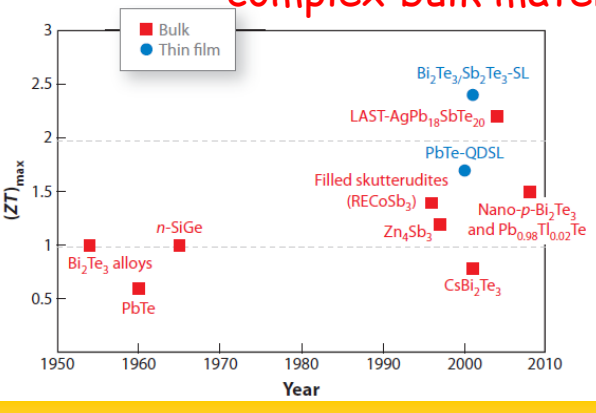

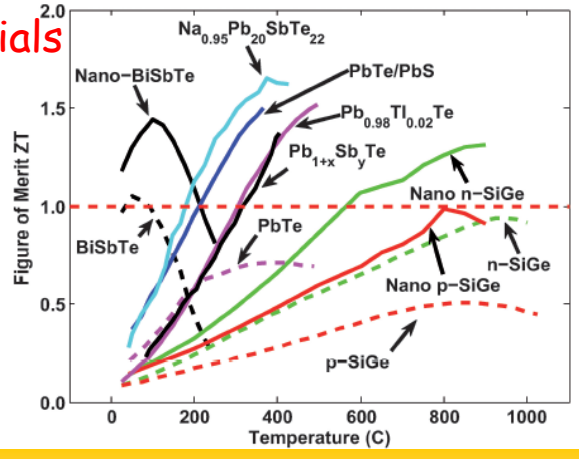

Mahan-Sofo mechanism

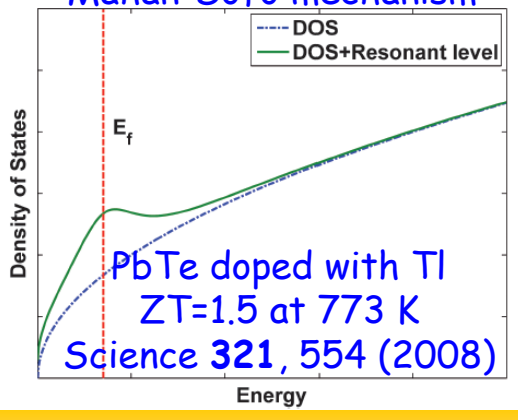

PbTe doped with Tl
ZT=1.5 at 773 K
Science **321**, 554 (2008)

New Routes for ZT Optimization Brought by Low-Dimensional and Nanoscale Devices

Transmission peaks or nodes

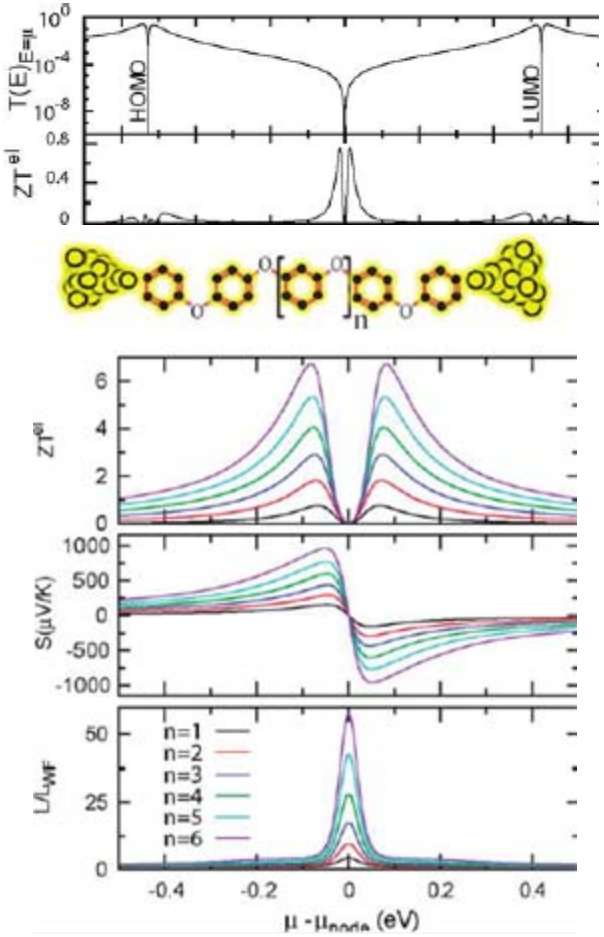

ACS Nano **4**, 5314 (2010)

$$L = \kappa_{el}/GT$$

$$L_{WF} = \pi^2/3(k_B/e)^2$$

Coulomb interaction

PRB **78**, 161406(R) (2008)

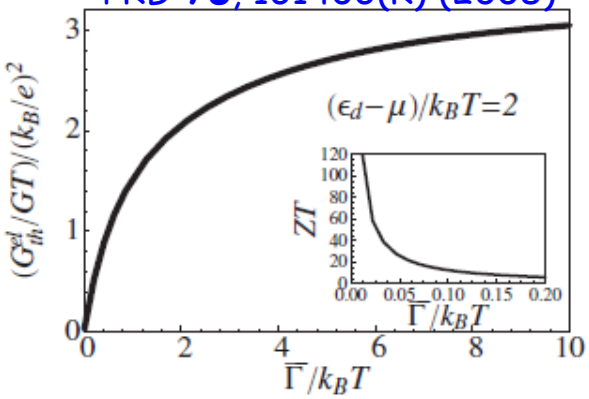

Nonlinear regime

PRB **82**, 045412 (2010)

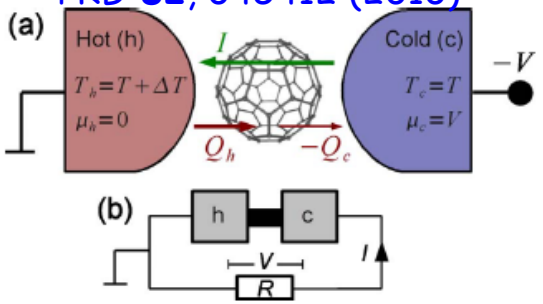

$$\eta = IV/Q_h$$

Electron-phonon coupling

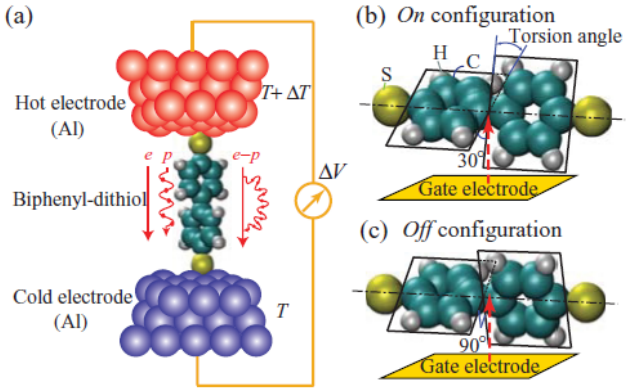

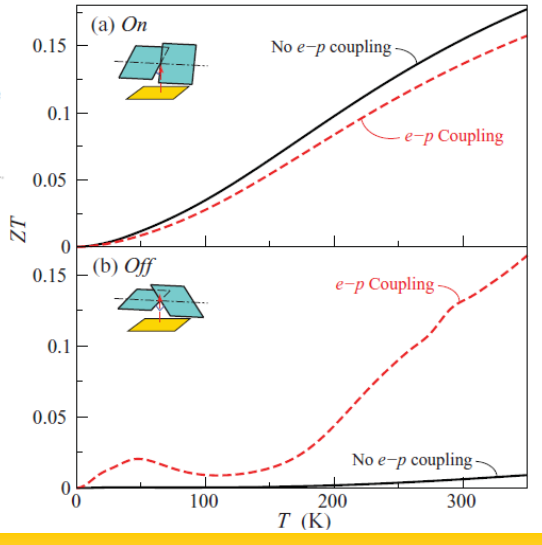

PR B **83**, 195415 (2011)

Graphene as a Building Block of Nanoscale and Low-Dimensional Devices

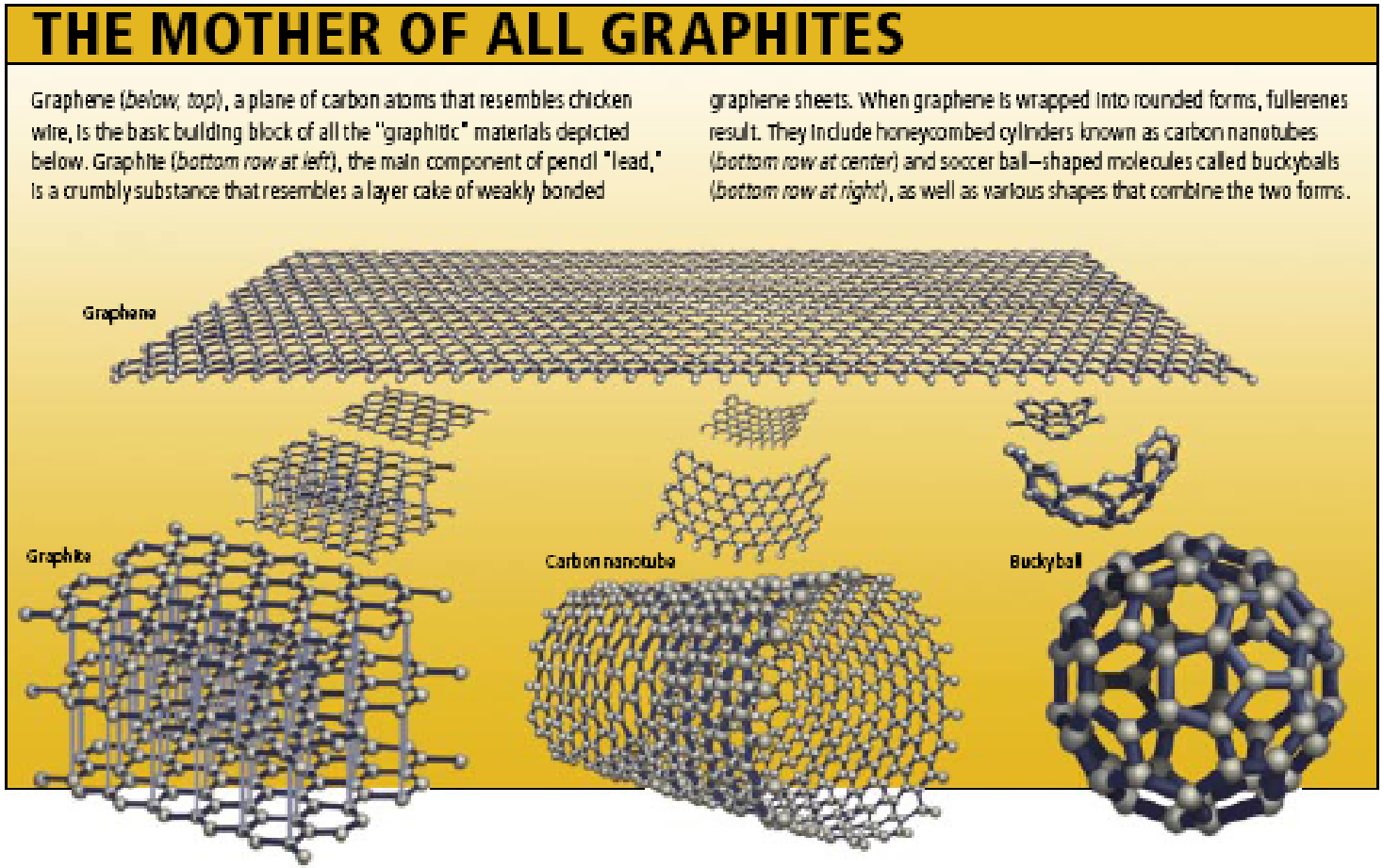

Large-Area Graphene is not Suitable for Thermoelectric Applications

Balandin Lab, New J. Phys. **11**, 095012 (2009)

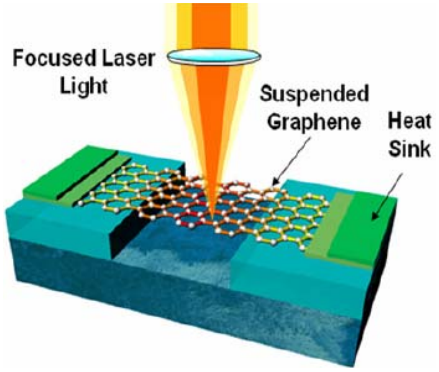

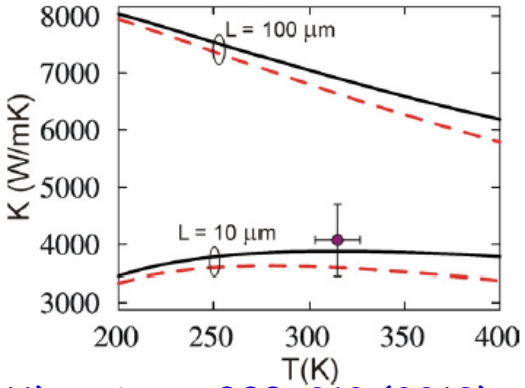

Kim Lab, PRL **102**, 096807 (2009)

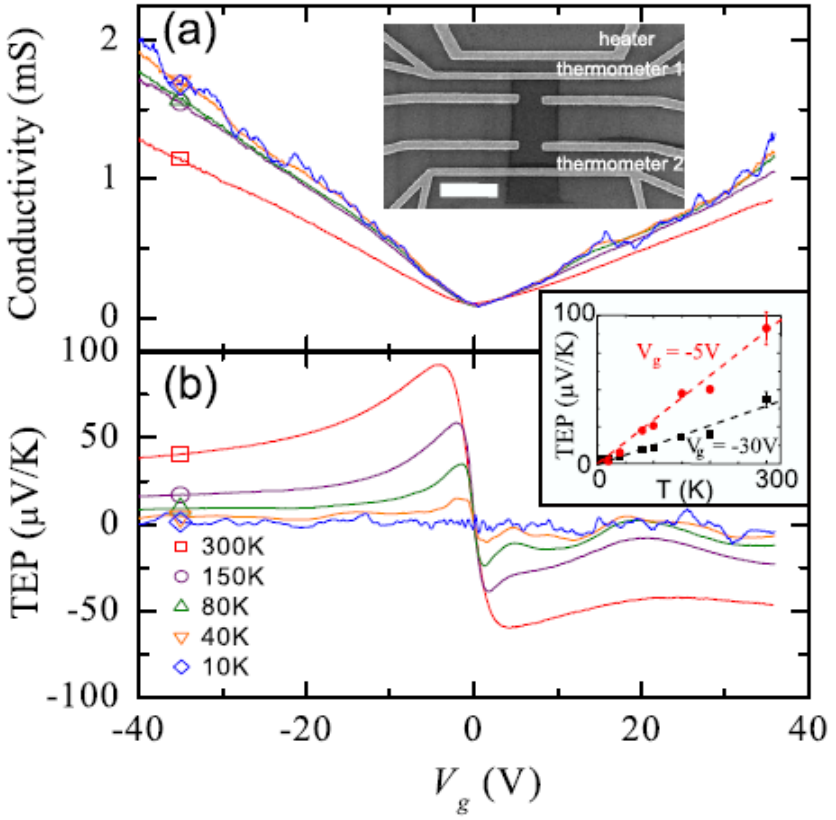

Shi Lab, *ACS Nano* **5**, 321 (2011); *Science* **328**, 213 (2010)

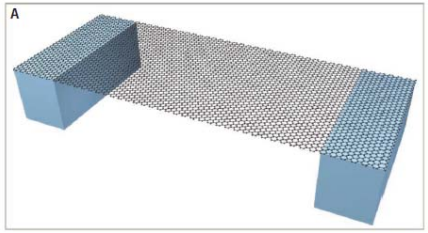

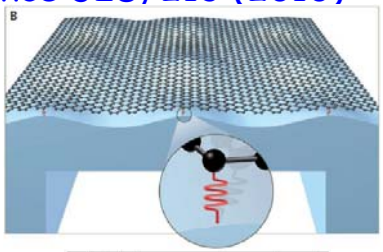

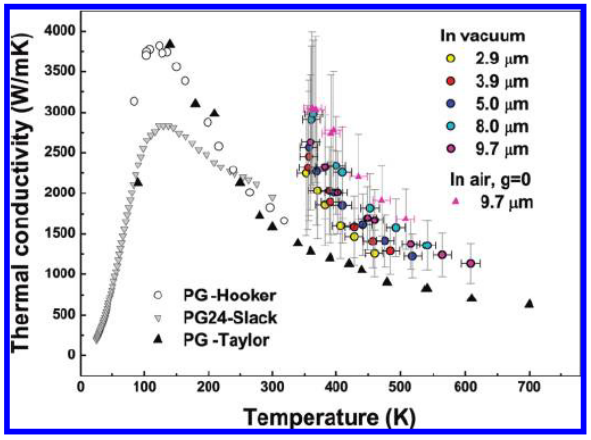

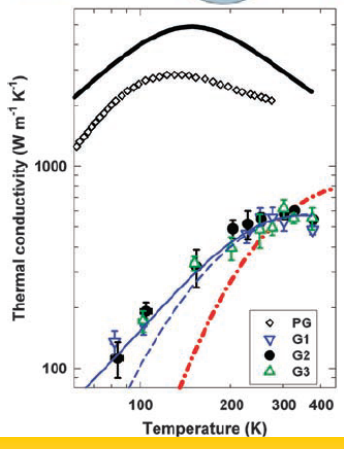

nature materials
REVIEW ARTICLE
PUBLISHED ONLINE: 22 JULY 2011 | DOI: 10.1038/NMAT3064

Thermal properties of graphene and nanostructured carbon materials

Alexander A. Balandin

Zigzag and Chiral GNRs with Nanopore Arrays as Potentially High-ZT Thermoelectrics

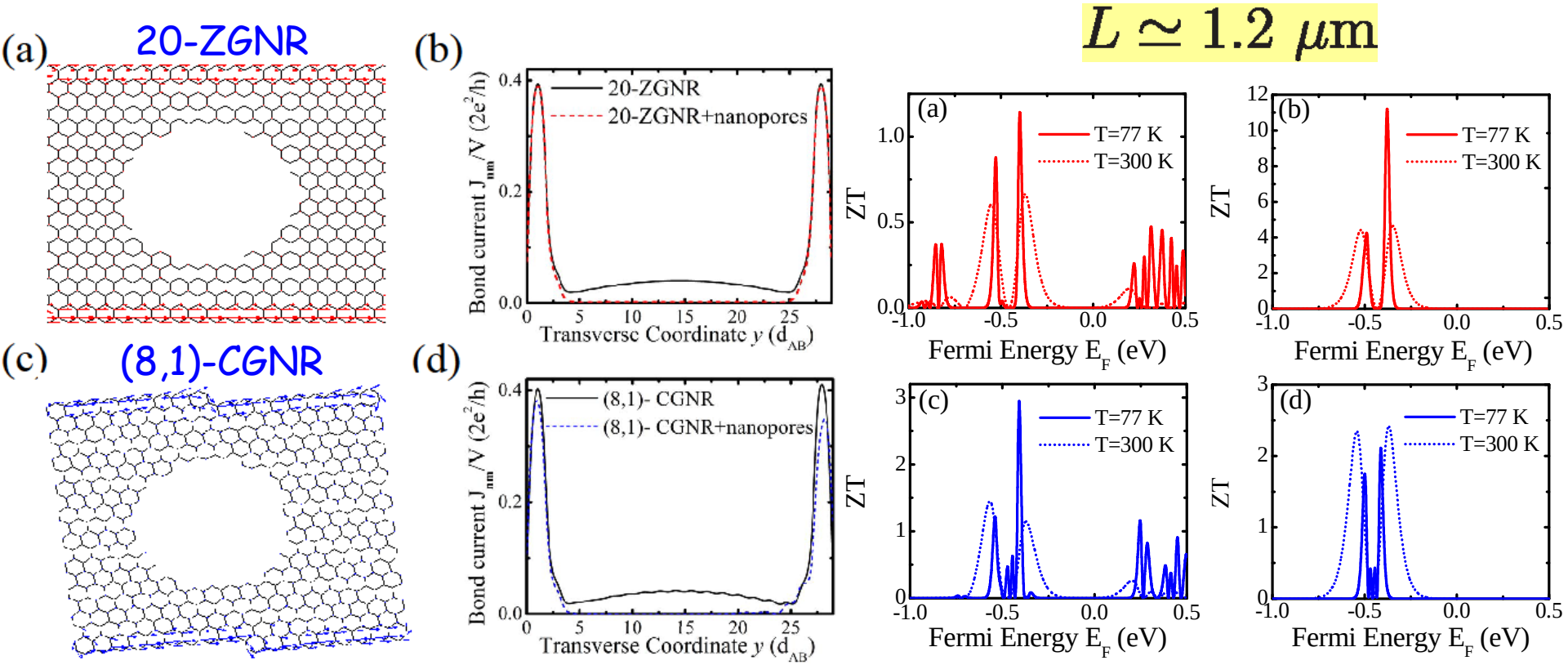

Nikolic group, arXiv:1201.1665

NEGF Fundamentals

Basic NEGF quantities:

density of available quantum states:

$$G^r_{\sigma\sigma'}(t,t') = -\frac{i}{\hbar}\Theta(t-t')\langle\{\hat{c}_{\mathbf{r}\sigma}(t), \hat{c}^\dagger_{\mathbf{r}'\sigma'}(t')\}\rangle$$

how are those states occupied:

$$G^<_{\sigma\sigma'}(t,t') = \frac{i}{\hbar}\langle\hat{c}^\dagger_{\mathbf{r}'\sigma'}(t')\hat{c}_{\mathbf{r}\sigma}(t)\rangle$$

NEGFs for steady-state transport:

$$G^r(t,t') \to G^r(t-t') \xrightarrow{\text{FT}} G^r(E) \qquad G^<(t,t') \to G^<(t-t') \xrightarrow{\text{FT}} G^<(E)$$

$$\boldsymbol{D}_{\text{eq}} = -\frac{1}{\pi}\int_{-\infty}^{+\infty} dE\, \text{Im}\,\mathbf{G}^r(E) f(E-E_F) \qquad \boldsymbol{D}_{\text{neq}} = \frac{1}{2\pi i}\int_{-\infty}^{+\infty} dE\, \mathbf{G}^<(E)$$

NEGF (quantum) vs. Boltzmann (semiclassical) nonequilibrium statistical mechanics:

$$\begin{aligned} G^r(E) &= [E - H - \Sigma^r_{\text{leads}} - \Sigma^r_{\text{int}}]^{-1} \\ G^<(E) &= G^r(E)[\Sigma^<_{\text{leads}}(E) + \Sigma^<_{\text{int}}(E)]G^a(E) \end{aligned}$$

$$\mathbf{v}\cdot\nabla f + \mathbf{F}\cdot\nabla_{\mathbf{k}} f = I_{\text{coll}}[f]$$

$$\mathbf{j} = 2_s e\int \frac{d^3\mathbf{k}}{(2\pi)^3}\mathbf{v}(\mathbf{k}) f(\mathbf{k})$$

NEGF-based current expression for two-terminal nanostructures:

$$I_\alpha = \frac{2e}{h}\int dE\, \text{Tr}\,\{\Sigma^<_\alpha(E)G^>(E) - \Sigma^>_\alpha(E)G^<(E)\}$$

Meir-Wingreen formula

$$I(V_{ds}) = \frac{2e}{h}\int_{-\infty}^{+\infty} dE\, \text{Tr}\,\{\mathbf{\Gamma}_R(E,V_{ds})\mathbf{G}^r_{S1}\mathbf{\Gamma}_L(E,V_{ds})\mathbf{G}^a_{1S}\}\,[f(E-\mu_L)-f(E-\mu_R)]$$

Landauer-Büttiker-type formula (phase-coherent transport where Coulomb interaction is treated at the mean-field level)

Electronic Thermopower, Conductance and Thermal Conductance via NEGF

- Electronic transmission and its integrals:

$$\begin{aligned}
\mathcal{T}_{\rm el}(E) &= {\rm Tr}\left\{\mathbf{\Gamma}_R(E)\mathbf{G}(E)\mathbf{\Gamma}_L(E)\mathbf{G}^\dagger(E)\right\} \\
\mathbf{G}(E) &= [E\mathbf{S}-\mathbf{H}-\mathbf{\Sigma}_L(E)-\mathbf{\Sigma}_R(E)]^{-1} \\
H_{ij} &= \langle\phi_i|\hat{H}_{\rm KS}|\phi_j\rangle,\ S_{ij}=\langle\phi_i|\phi_j\rangle \\
\mathbf{\Gamma}_{L,R}(E) &= i[\mathbf{\Sigma}_{L,R}(E)-\mathbf{\Sigma}^\dagger_{L,R}(E]
\end{aligned}$$

$$K_n(\mu)=\frac{2}{h}\int_{-\infty}^{\infty} dE\,\mathcal{T}_{\rm el}(E)(E-\mu)^n\left(-\frac{\partial f(E,\mu)}{\partial E}\right)$$

- Electronic conductance, thermopower, and thermal conductance:

$$G=e^2K_0(\mu)$$

$$S=K_1(\mu)/[eTK_0(\mu)]$$

$$\frac{-\partial f(E,\mu)}{\partial E}=\{2k_BT[1+\cosh(E-\mu)/k_BT]\}^{-1}$$

$$\kappa_{\rm el}=\{K_2(\mu)-[K_1(\mu)]^2/K_0(\mu)\}/T$$

Nikolić group, J. Comp. Electronics **11**, 78 (2012)

Third-Nearest-Neighbor π-Orbital Tight-Binding Hamiltonian For Graphene

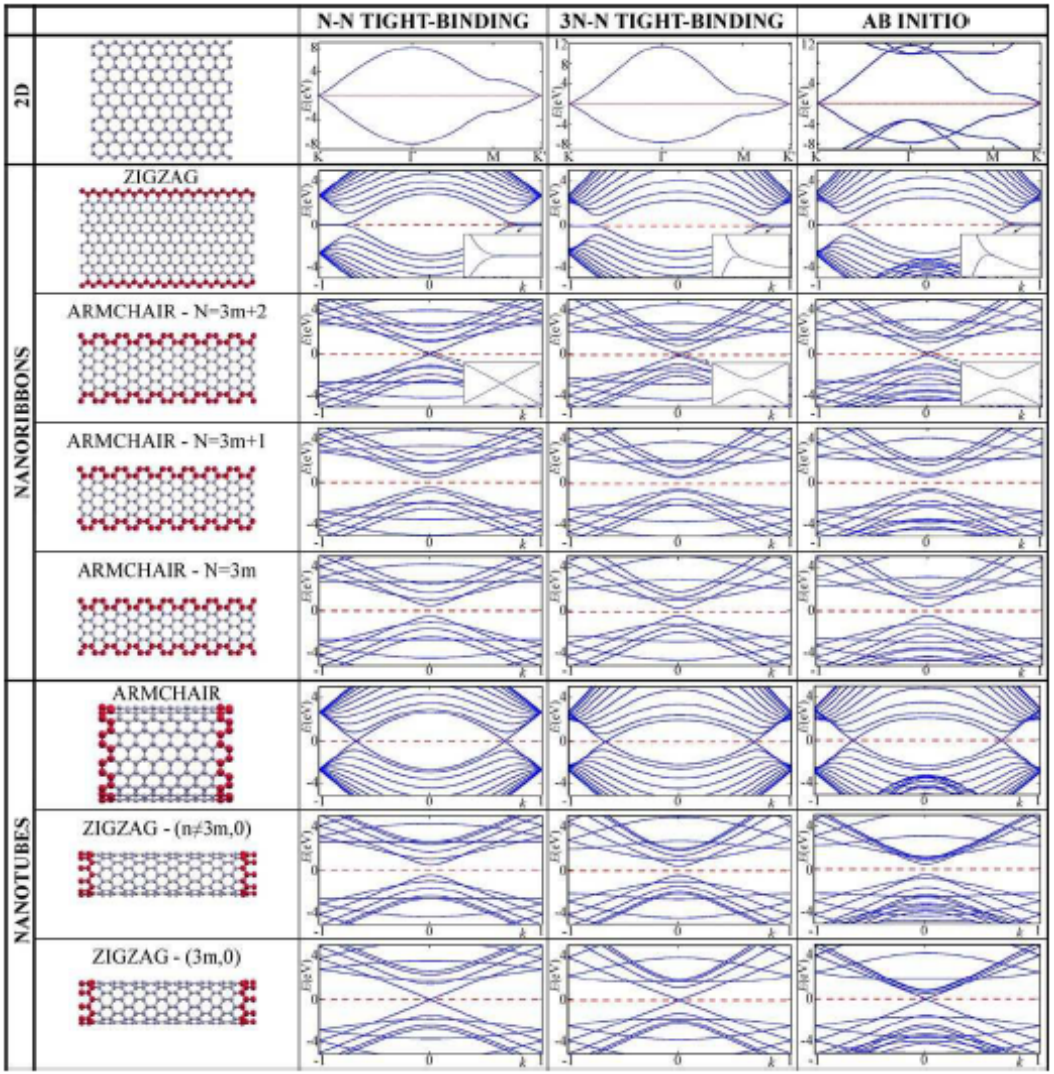

Nano Research **1**, 361 (2008)

$$\hat{H} = \sum_{\mathbf{n}} \varepsilon_{\mathbf{n}} \hat{c}^{\dagger}_{\mathbf{n}} \hat{c}_{\mathbf{n}} - \sum_{\mathbf{n},\mathbf{m}} t^{\mathbf{m}}_{\mathbf{n}} \hat{c}^{\dagger}_{\mathbf{n}} \hat{c}_{\mathbf{m}}$$

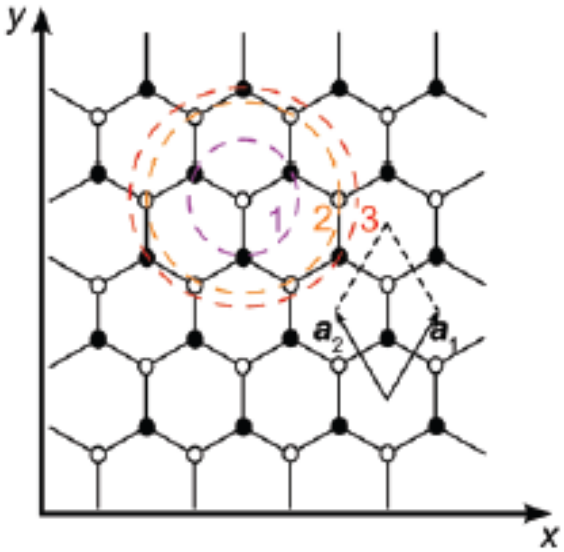

$$t^{\mathbf{n}+\mathbf{d}_{AB}}_{\mathbf{n}} = 2.7 \text{ eV}$$
$$t^{\mathbf{n}+\mathbf{d}_{AA}}_{\mathbf{n}} = t^{\mathbf{n}+\mathbf{d}_{BB}}_{\mathbf{n}} = 0.2 \text{ eV}$$
$$t^{\mathbf{n}+\mathbf{d}_{AB'}}_{\mathbf{n}} = 0.18 \text{ eV}$$

Zigzag GNR: Fundamentals

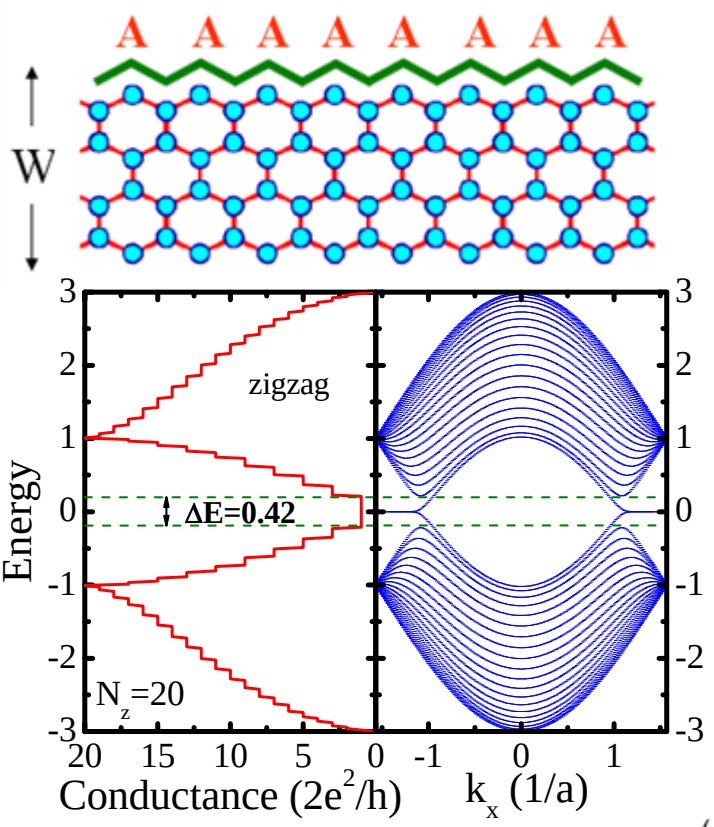

Areshkin & White,
Nano Lett. **7**, 3253 (2007)

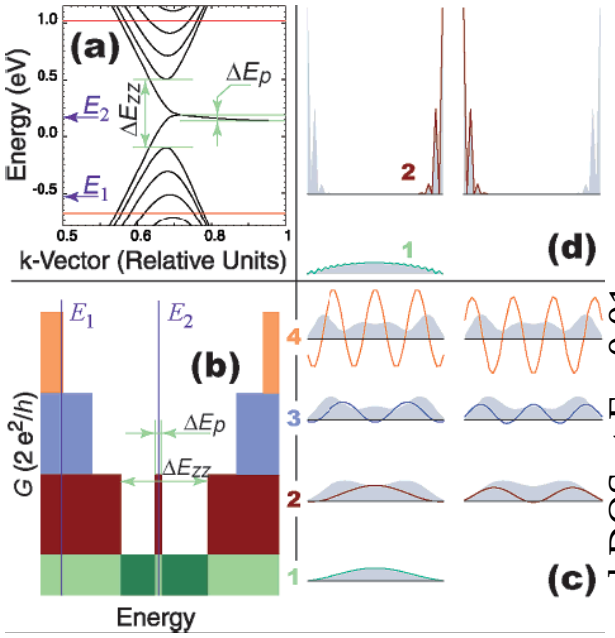

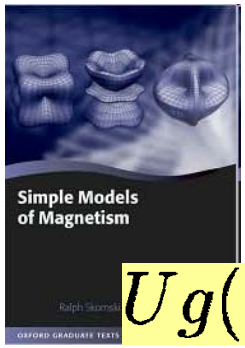

$$Ug(E_F) > 1$$

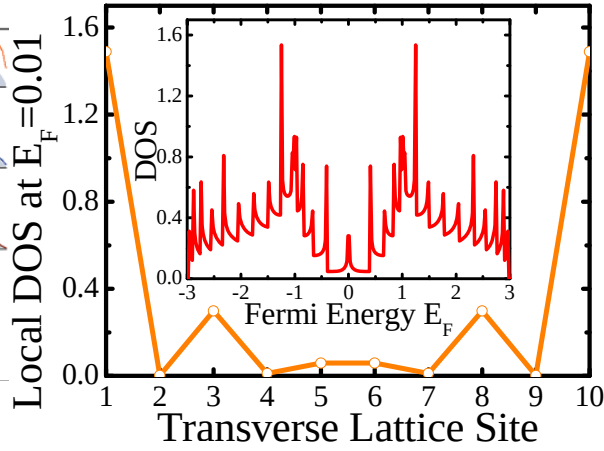

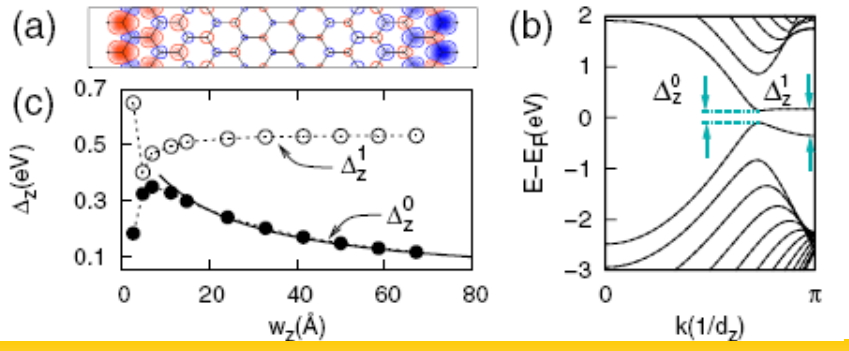

Son, Cohen, and Louie,
PRL **97**, 216803 (2006)

First-Principles Quantum Transport Modeling Charge, Heat and Spin Transport: NEGF+DFT

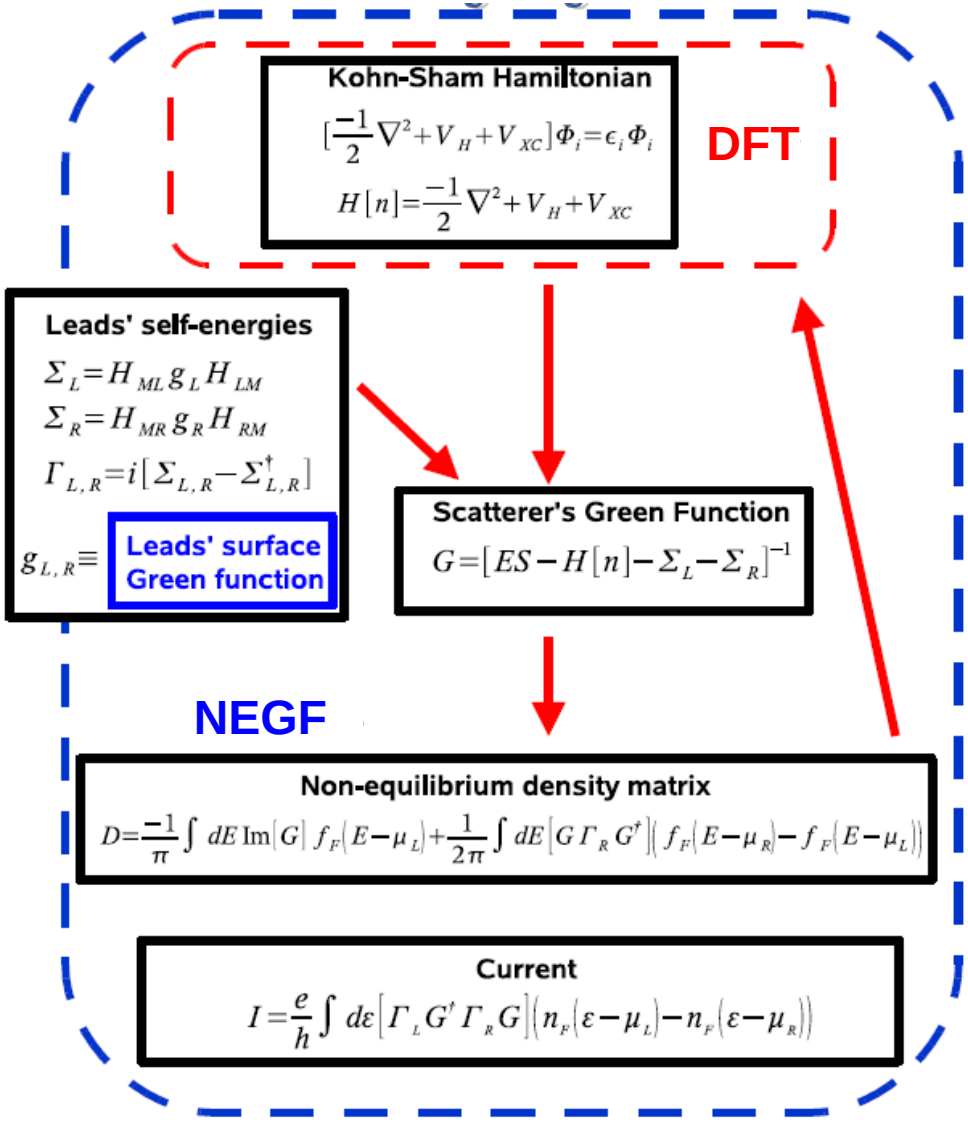

open source

commercial

GPAW!

Smeagol
Non-equilibrium Electronic Transport

Trans siesta

ALACANT
ALicante Ab initio Computation Applied to NanoTransport

QuantumWise

NANODCAL

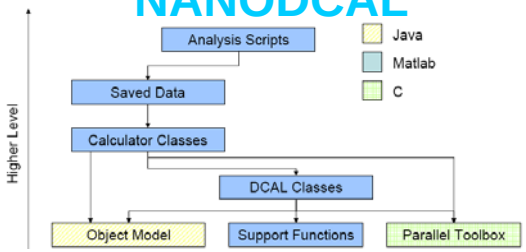

How to Apply NEGF-DFT to Devices Containing Thousands of Atoms

Main Obstacles: Computational complexity $O(N^3)$ of matrix inversion to get the retarded GF and hard-to-converge real-axis integration of spiky NEGF expressions to get the density matrix

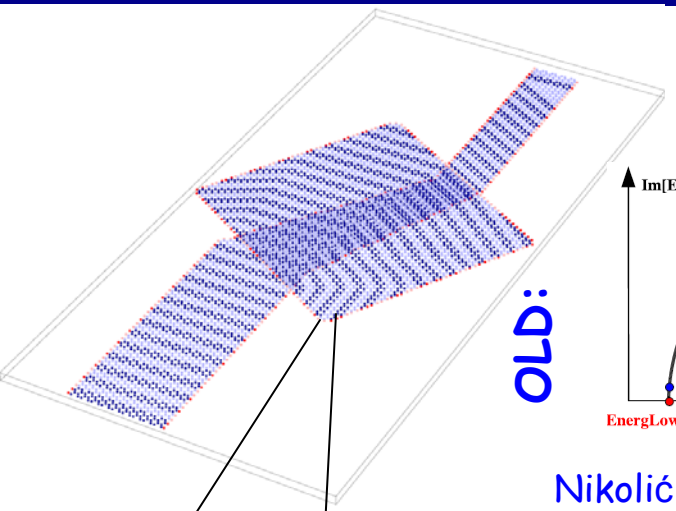

$\mathbf{H}_{i,i}$ $\mathbf{H}_{i+1,i+1}$

$\mathbf{H}_{i,i+1}$

Construct the layer retarded Green functions needed for charge density using recursive algorithms with O(N) complexity

OLD:

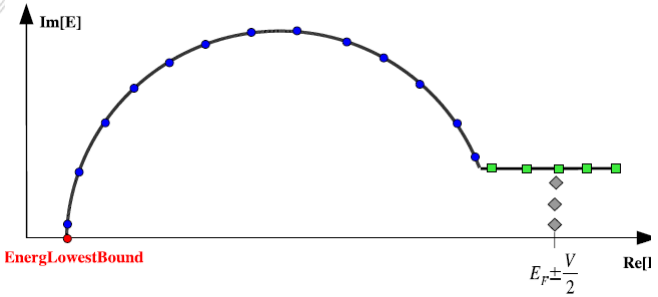

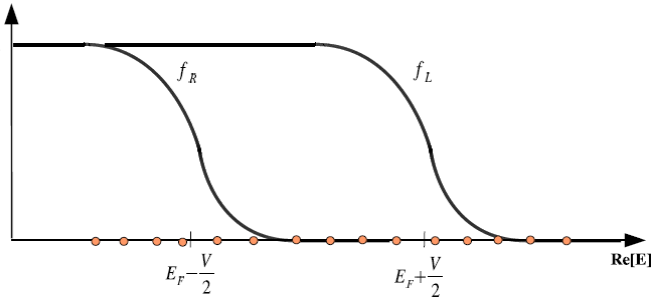

Nikolić group, PRB **81**, 155450 (2010)

$$\boldsymbol{\rho}_{\mathrm{eq}} = -\frac{1}{\pi}\mathrm{Im}\left[\sum_{j=1}^{N_{\mathrm{pole}}} 2\pi i \ \mathrm{Res}\left[\tilde{f}(z)\right]_{z=Z_j} \mathbf{G}^r(Z_j)\right],$$

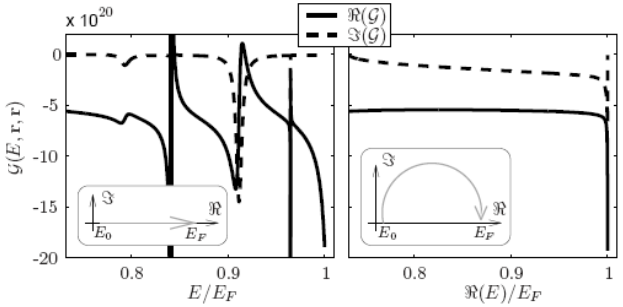

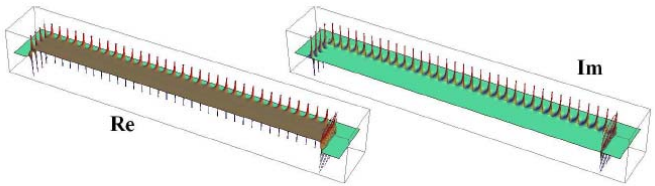

NEW:

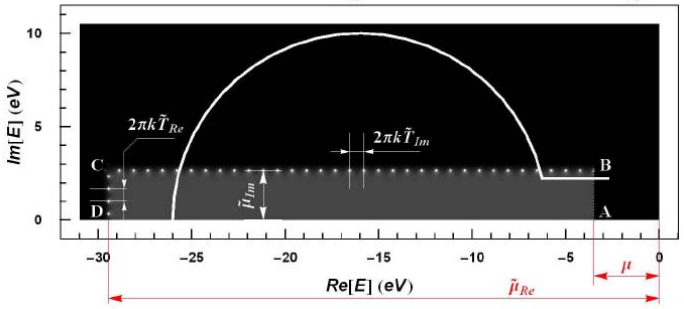

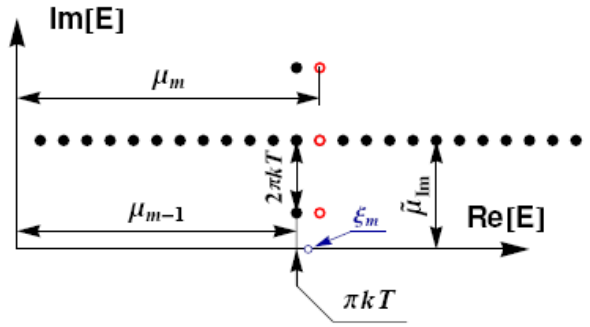

Gate Voltage Effect in All Carbon-Hydrogen GNRFET Composed of ~7000 Atoms

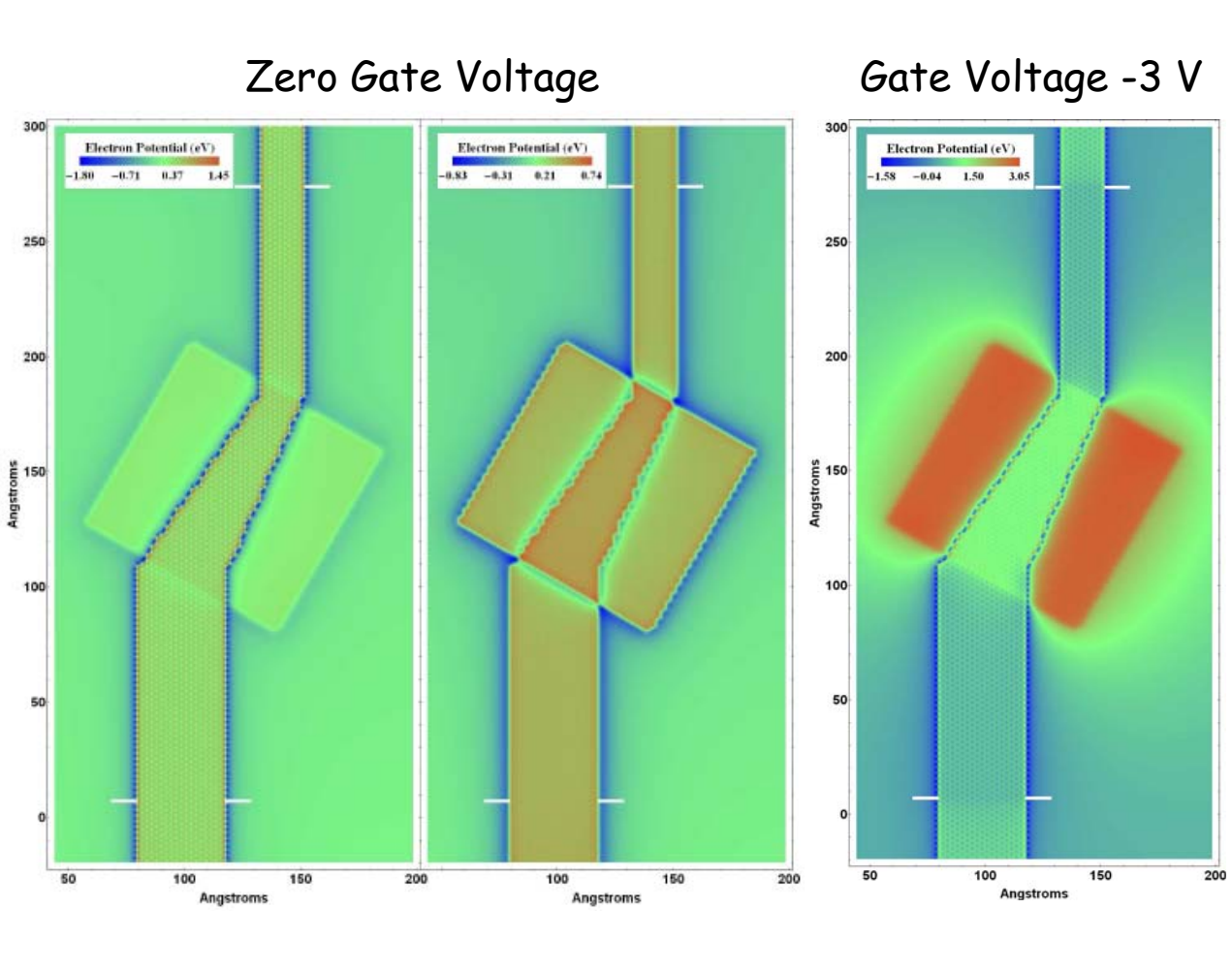

Nikolić group, PRB **81**, 155450 (2010)

NEGF-DFT For Multiterminal Devices

Saha et al., J. Chem. Phys. **131**, 164105 (2009)

$$D = -\frac{1}{\pi}\int_{-\infty}^{\infty} dE\,\mathrm{Im}\left[\mathrm{G}(E)f(E-\mu_m)\right] + \sum_{j\neq m}\int_{-\infty}^{\infty} dE\,\rho^j(E)\left[f(E-\mu_j)-f(E-\mu_m)\right]$$

$$\rho^i = \mathrm{G}(E)\Gamma_i(E)\mathrm{G}^\dagger$$

$$\tilde{D} = D^1 + \Delta^{12} + \Delta^{13}$$

$$D^1 = -\frac{1}{\pi}\int_{-\infty}^{\infty} dE\,\mathrm{Im}\left[G(E)\,f(E-\mu_1)\right]$$

$$\Delta^{12} = \int_{-\infty}^{\infty} dE\,\rho^2(E)\left[f(E-\mu_2)-f(E-\mu_1)\right]$$

$$\Delta^{13} = \int_{-\infty}^{\infty} dE\,\rho^3(E)\left[f(E-\mu_3)-f(E-\mu_1)\right]$$

$$\tilde{D} = D^2 + \Delta^{21} + \Delta^{23} \quad \cdots\ \cdots\ \cdots$$

$$D^2 = -\frac{1}{\pi}\int_{-\infty}^{\infty} dE\,\mathrm{Im}\left[G(E)\,f(E-\mu_2)\right]$$

$$\Delta^{21} = \int_{-\infty}^{\infty} dE\,\rho^1(E)\left[f(E-\mu_1)-f(E-\mu_2)\right]$$

$$\Delta^{23} = \int_{-\infty}^{\infty} dE\,\rho^3(E)\left[f(E-\mu_3)-f(E-\mu_2)\right]$$

$$D = w^1\left(D^1+\Delta^{12}+\Delta^{13}\right) + w^2\left(D^2+\Delta^{21}+\Delta^{23}\right) + w^3\left(D^3+\Delta^{31}+\Delta^{32}\right)$$

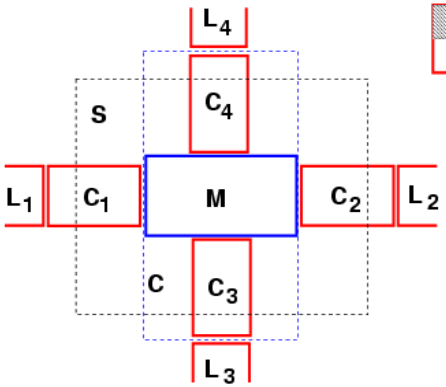

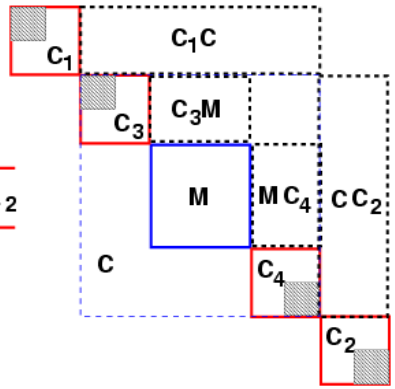

$$H = \begin{pmatrix} H_{C_1}+\Sigma_{\mu_1} & 0 & V_{C_1M} & 0 & 0 \\ 0 & H_{C_3}+\Sigma_{\mu_3} & V_{C_3M} & 0 & 0 \\ V_{MC_1} & V_{MC_3} & H_M & V_{MC_4} & V_{MC_2} \\ 0 & 0 & V_{C_4M} & H_{C_4}+\Sigma_{\mu_4} & 0 \\ 0 & 0 & V_{C_2M} & 0 & H_{C_2}+\Sigma_{\mu_2} \end{pmatrix}$$

$$I_\alpha = \frac{2e}{h}\sum_{\beta\neq\alpha}\int dE\,T(E,V_\beta,V_\alpha)[f(E-\mu_\beta)-f(E-\mu_\alpha)]$$

Phonon Thermal Conductance via NEGF Coupled to Minimal Force Constant 4NNN Model

❑Phonon conductance:

$$\kappa_{\rm ph} = \frac{\hbar^2}{2\pi k_B T^2} \int_0^\infty d\omega\, \omega^2 \mathcal{T}_{\rm ph}(\omega) \frac{e^{\hbar\omega/k_BT}}{(e^{\hbar\omega/k_BT}-1)^2}$$

$$\mathcal{T}_{\rm ph}(\omega) = {\rm Tr}\left\{\mathbf{\Lambda}_L(\omega)\mathbf{G}(\omega)\mathbf{\Lambda}_R(\omega)\mathbf{G}^\dagger(\omega)\right\}$$
$$\mathbf{G}(\omega) = [\omega^2\mathbf{M} - \mathbf{K} - \mathbf{\Pi}_L(\omega) - \mathbf{\Pi}_R(\omega)]^{-1}$$

❑Why no phonon-phonon scattering? $W \ll \ell \approx 677$ nm at 300 K [APL **98**, 141919 (2011)]

❑Empirical 4NNN force constant matrix:

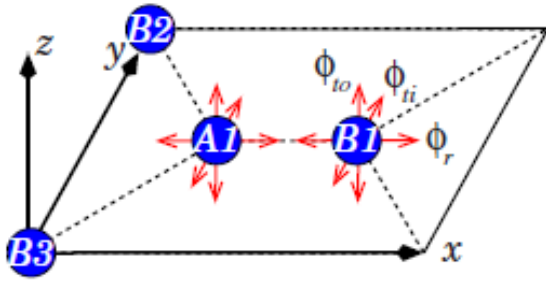

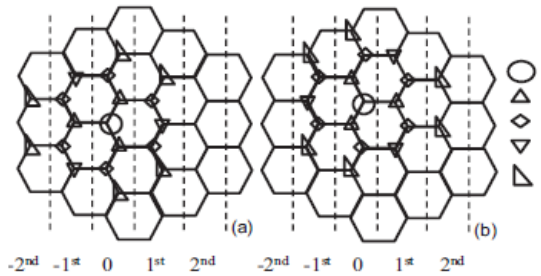

$$K_{A1,n} = \begin{pmatrix} \phi_{\rm r}^{(n)} & 0 & 0 \\ 0 & \phi_{\rm ti}^{(n)} & 0 \\ 0 & 0 & \phi_{\rm to}^{(n)} \end{pmatrix}$$

TABLE I. Force-constant parameters for graphene in units of 10^4 dyn/cm=10 N/m.

	Parameters by Saito *et al.* (Ref. 38)			Our parametrization		
Neighbor shell	$\phi_{\rm r}^{(n)}$	$\phi_{\rm ti}^{(n)}$	$\phi_{\rm to}^{(n)}$	$\phi_{\rm r}^{(n)}$	$\phi_{\rm ti}^{(n)}$	$\phi_{\rm to}^{(n)}$
First	36.50	24.50	9.82	41.8	15.2	10.2
Second	8.80	−3.23	−0.40	7.6	−4.35	−1.08
Third	3.00	−5.25	0.15	−0.15	3.39	1.0
Fourth	−1.92	2.29	−0.58	−0.69	−0.19	−0.55

$$\phi_t^{(1)} + 6\phi_t^{(2)} + 4\phi_t^{(3)} + 14\phi_t^{(4)} = 0$$

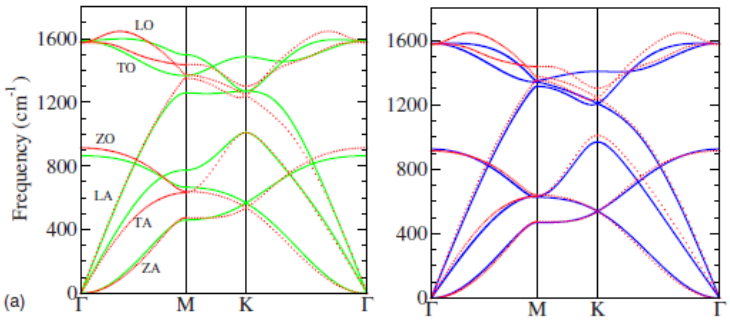

PRB **78**, 045410 (2008)

Phonon Thermal Conductance via NEGF Coupled to Brenner Empirical Potential or DFT

- Brenner empirical interatomic potential for hydrocarbon systems (GULP or GPAW):

PRB **81**, 205441 (2010)

$$V_{ij} = f_{ij}^C(f_{ij}^R - \bar{b}_{ij} f_{ij}^A), \quad \bar{b}_{ij} = \frac{1}{2}(b_{ij}^{\sigma-\pi} + b_{ji}^{\sigma-\pi}) + \Pi_{ij}^{RC} + b_{ij}^{DH},$$

$$f_{ij}^R = \left(1 + \frac{Q}{r_{ij}}\right) A e^{-\alpha r_{ij}}, \qquad b_{ij}^{\sigma-\pi} = \left(1 + \sum_{k \neq i,j} f_{ik}^C g_{ijk}\right)^{-1/2},$$

$$f_{ij}^A = \sum_{n}^{3} B_n e^{-\lambda_n r_{ij}}, \qquad g_{iik} = \sum^{5} \beta_i \cos^i[\theta_{ijk}].$$

$$b_{ij}^{DH} = \frac{T_0}{2} \sum_{k,l \neq i,j} f_{ik}^C f_{jl}^C (1 - \cos^2[\Theta_{ijkl}])$$

$$K_{I\alpha,J\beta} = \partial V / (\partial R_{I\alpha} \partial R_{J\beta})$$

The Brenner EIPs are short range, so they cannot accurately fit the graphene dispersion over the entire BZ. However, the thermal transport depends more sensitively on the accuracy of acoustic phonon frequencies near the zone center where the longitudinal- and transverse-acoustic (LA and TA) velocities and the quadratic curvature of the out-of-plane acoustic (ZA) branch are determined. Conversely, only weak thermal excitation of the optical phonons and acoustic phonons near the BZ boundary occurs around room temperature because of the large Debye temperature (~ 2000 K) of graphene.

- First-principles brute force method to obtain the force constant matrix (GPAW):

we displace each atom I by $Q_{I\alpha}$ in the direction α={x,y,z} to get the forces $F_{I\alpha,J\beta}$ on atom J≠ I in direction β

$$K_{I\alpha,J\beta} = [F_{J\beta}(Q_{I\alpha}) - F_{J\beta}(-Q_{I\alpha})]/2Q_{I\alpha}$$

$$K_{I\alpha,I\beta} = -\Sigma_{J \neq I} K_{I\alpha,J\beta}$$

for intra-atomic elements impose momentum conservation

Which Method Should You Use: Minimal 4NNNFC vs. Brenner EIP vs. DFT

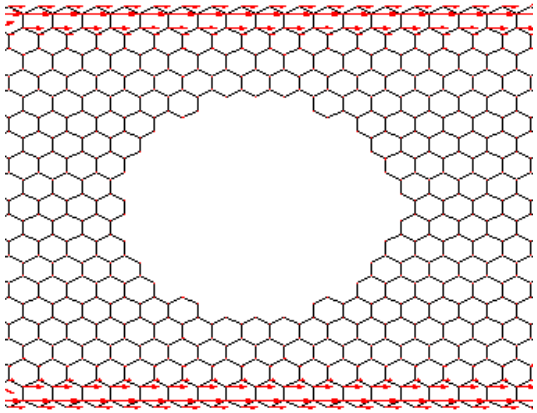

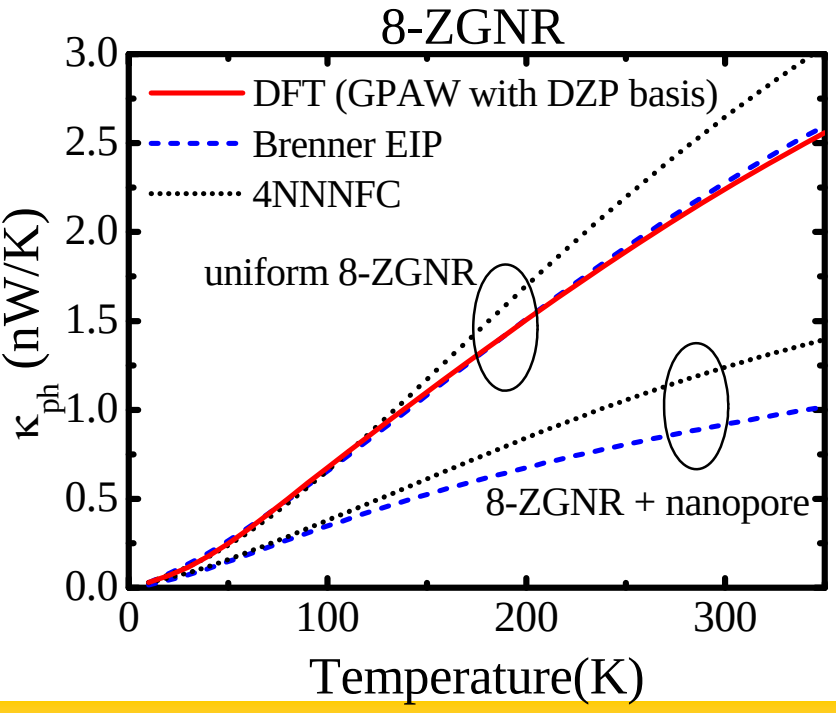

ZGNR|18-annulene|ZGNR

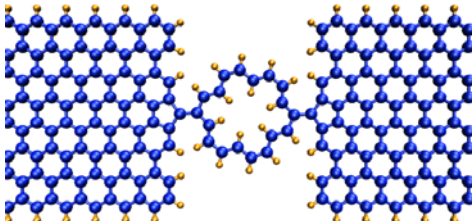

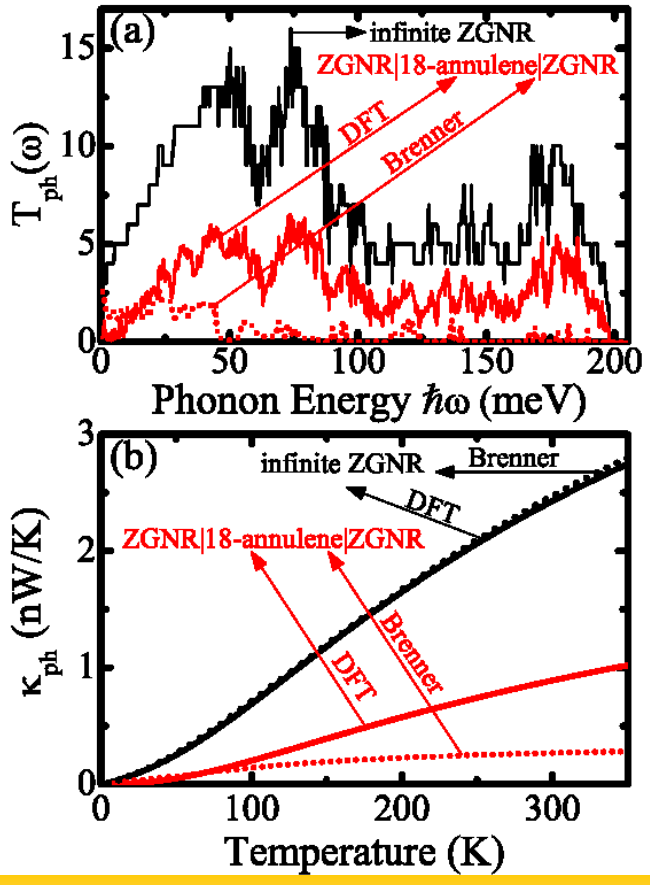

Coupled Electron-Phonon Transport via NEGF

$$\hat{H} = \hat{H}_{\mathrm{e}}^{0} + \hat{H}_{\mathrm{ph}}^{0} + \hat{H}_{\mathrm{e\text{-}ph}} = \sum_{i,j} H_{ij}^{0} \hat{c}_i^{\dagger} \hat{c}_j + \sum_{i,j} \hbar\omega_{\lambda} \hat{a}_{\lambda}^{\dagger} \hat{a}_{\lambda} + \sum_{\lambda,i,j} M_{ij}^{\lambda} \hat{c}_i^{\dagger} \hat{c}_j (\hat{a}_{\lambda}^{\dagger} + \hat{a}_{\lambda})$$

empirical models or DFT (GPAW) computed

(a)

$$\Sigma^{H} = i \sum_{\lambda} \frac{2}{\omega_{\lambda}} \int \frac{dE'}{2\pi} \mathbf{M}^{\lambda} \mathrm{Tr}\left[\mathbf{G}_0^{<}(E') \mathbf{M}^{\lambda}\right]$$

$$\Sigma^{H,<} = 0$$

(b)

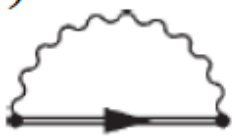

$$\Sigma^{F}(E) = i \sum_{\lambda} \int \frac{dE'}{2\pi} \mathbf{M}^{\lambda} \left[\begin{array}{l} \mathbf{D}_0(E-E') \mathbf{G}_0^{<}(E') + \mathbf{D}_0(E-E') \mathbf{G}_0(E') \\ + \mathbf{D}_0^{<}(E-E') \mathbf{G}_0(E') \end{array} \right] \mathbf{M}^{\lambda}$$

$$\Sigma^{F,<}(E) = i \sum_{\lambda} \int \frac{dE'}{2\pi} \mathbf{M}^{\lambda} \mathbf{D}_0(E-E') \mathbf{G}_0^{<}(E') \mathbf{M}^{\lambda}$$

electron self-energies in SCBA

(c)

$$\Pi(\omega) = -i \sum_{\lambda} \int \frac{dE'}{2\pi} \mathbf{M}^{\lambda} \left[\begin{array}{l} \mathbf{G}_0(E') \mathbf{G}_0^{<}(E'-\omega) + \\ \mathbf{G}_0^{<}(E) \mathbf{G}_0^{\dagger}(E'-\omega) \end{array} \right] \mathbf{M}^{\lambda}$$

$$\Pi^{<}(\omega) = -i \sum_{\lambda} \int \frac{dE'}{2\pi} \mathbf{M}^{\lambda} \mathbf{G}_0^{<}(E) \mathbf{G}_0^{>}(E'-\omega) \mathbf{M}^{\lambda}$$

phonon self-energies in SCBA

second-order diagrams

(d)

(e)

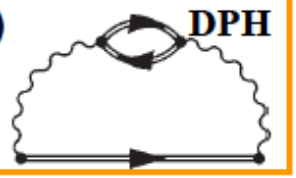

❑Phonon drag:

$S = S_{\mathrm{el}} + S_{\mathrm{ph}}$

arises due to interchange of momentum between acoustic phonons and electrons

❑Electron drag:

phonons are dragged by electrons from low into high T region

❑Three- and four-phonon many-body interactions

(a) (b) (c)

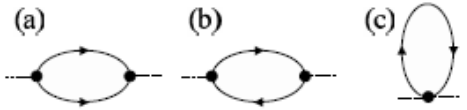

PRB 74, 125402 (2006)

Electron and Phonon Transport in ZGNRs and CGNRs with Nanopores

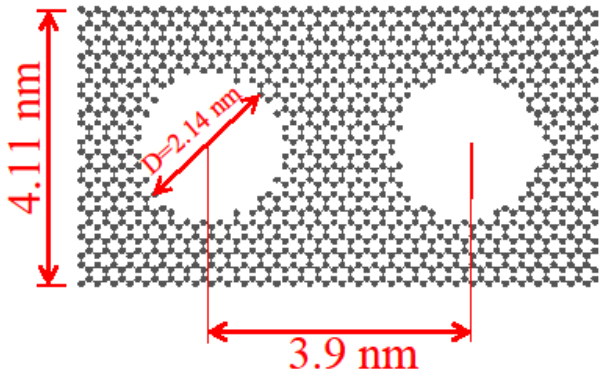

$L \simeq 1.2\ \mu\text{m}$

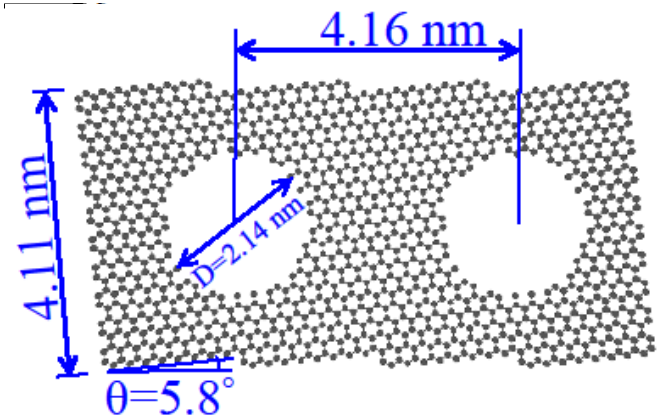

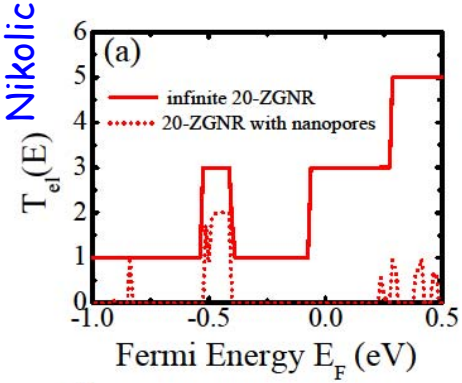

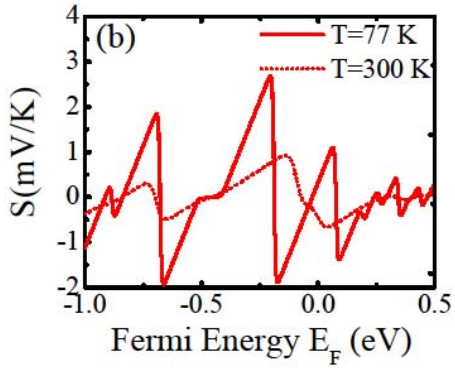

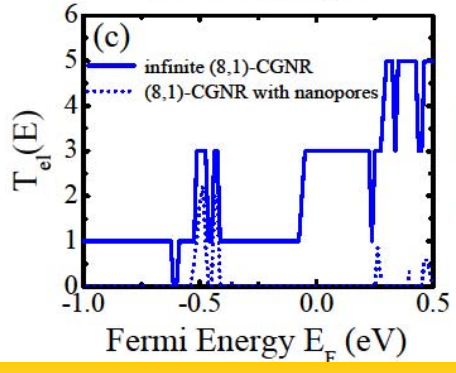

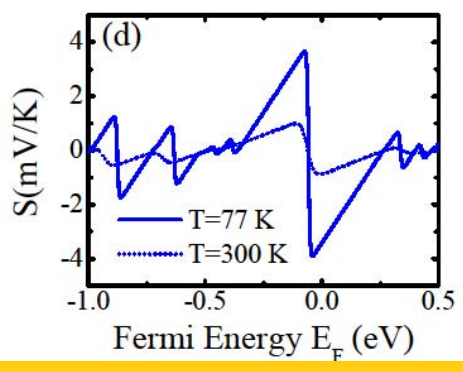

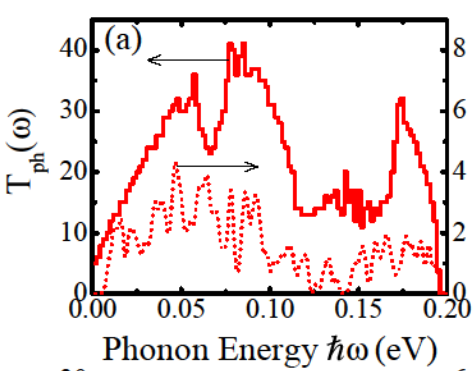

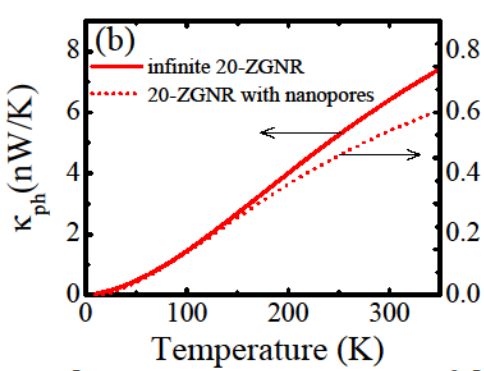

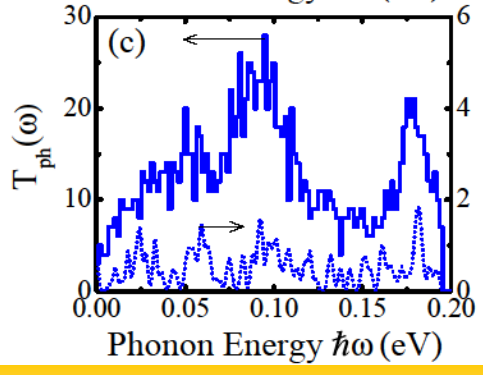

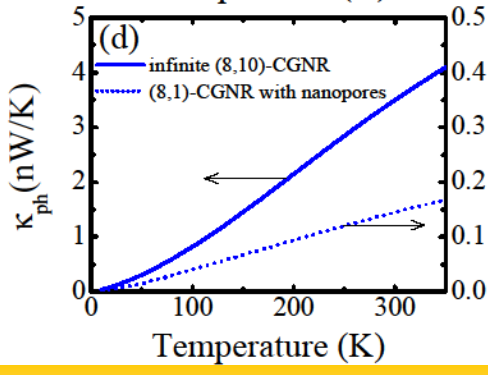

Graphene Nanoribbons: Fabrication

Science **319**, 1229 (2008): Chemical Derivation

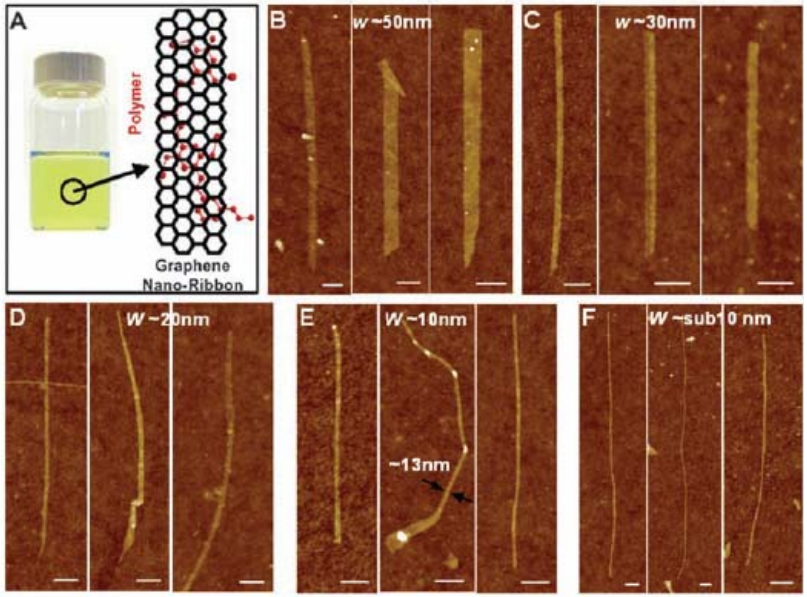

Nature **458**, 872 (2009): SWCNT Unzipping

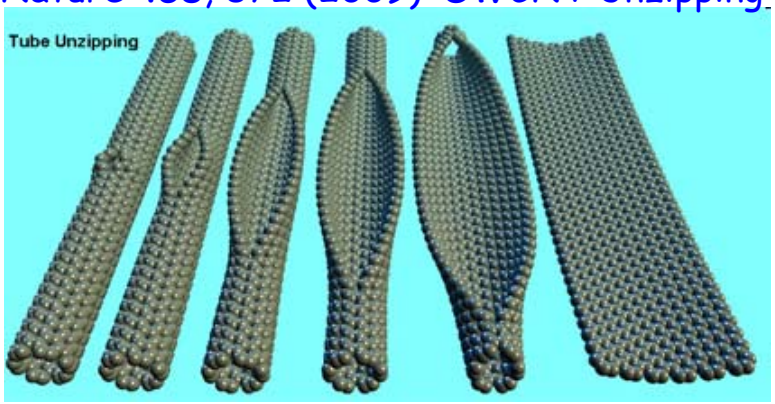

Nature Nanotech. **5**, 190 (2010): Graphene nanomesh

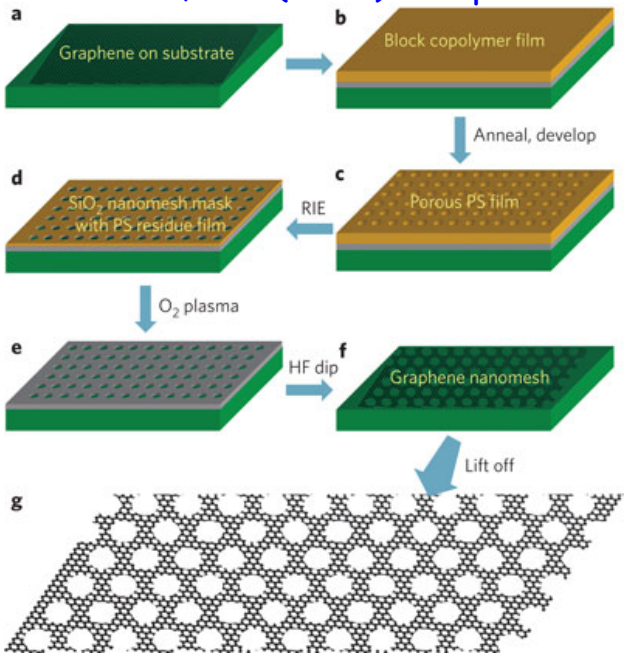

Nature Nanotech. **3**, 397 (2008): STM Nanolithography

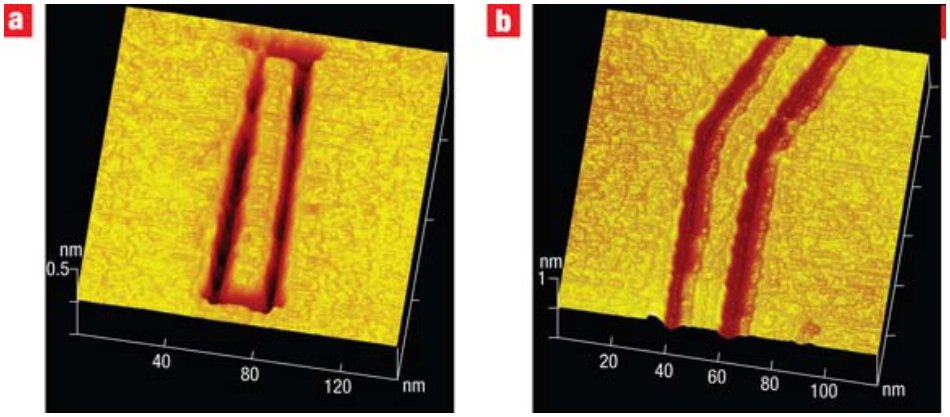

Band vs Transport Gaps in GNRs with Rough Edges

PHYSICAL REVIEW B 81, 193408 (2010)

Magnetotransport through graphene nanoribbons

Jeroen B. Oostinga,[1,2] Benjamin Sacépé,[1] Monica F. Craciun,[3] and Alberto F. Morpurgo[1]

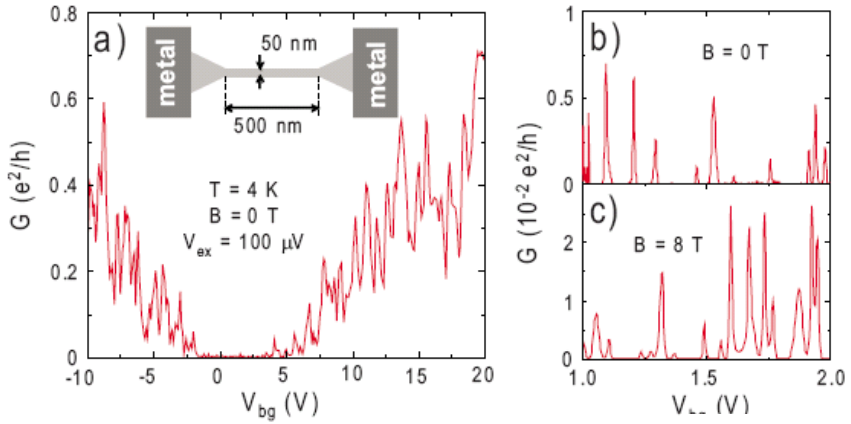

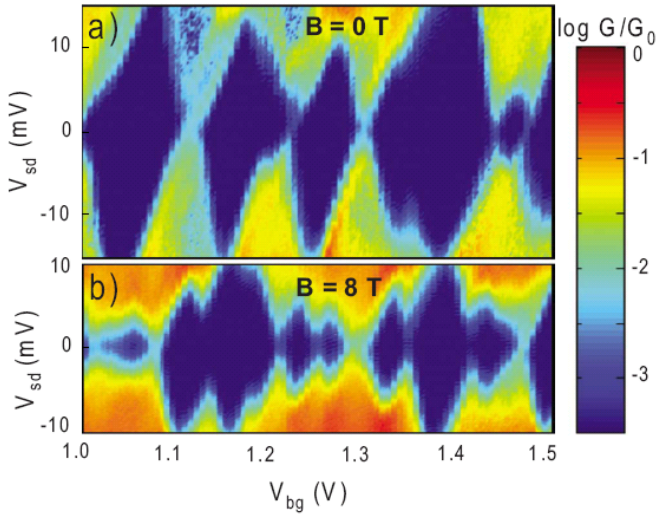

IOP Publishing
Semicond. Sci. Technol. 25 (2010) 034002 (7pp)
Semiconductor Science and Technology
doi:10.1088/0268-1242/25/3/034002

Energy and transport gaps in etched graphene nanoribbons

F Molitor, C Stampfer, J Güttinger, A Jacobsen, T Ihn and K Ensslin

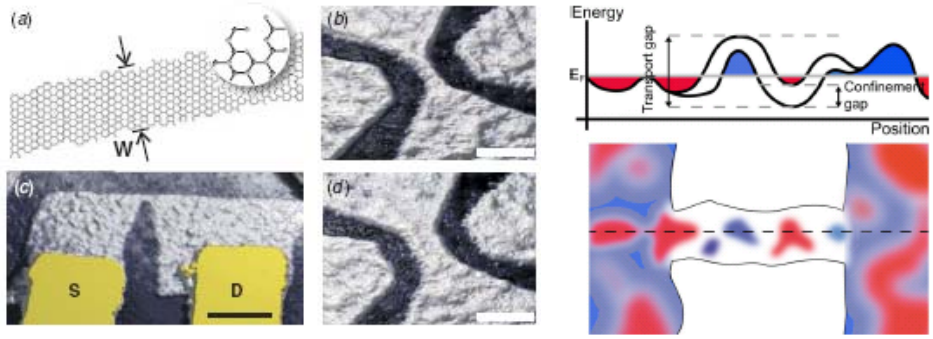

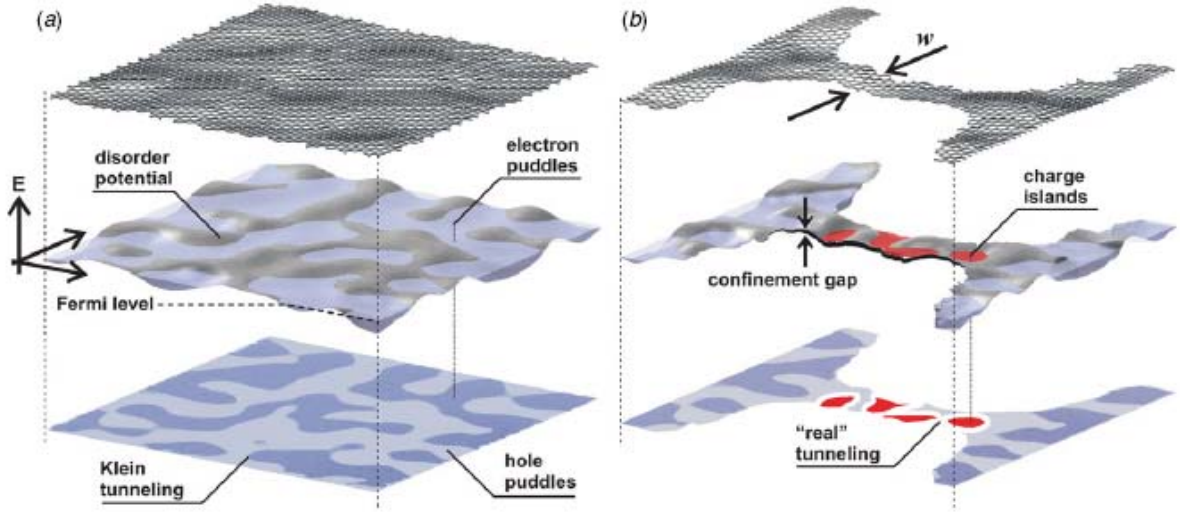

Can We Control Formation of GNR Edges?

SCIENCE VOL 323 27 MARCH 2009

Controlled Formation of Sharp Zigzag and Armchair Edges in Graphitic Nanoribbons

Xiaoting Jia,[1] Mario Hofmann,[2] Vincent Meunier,[3] Bobby G. Sumpter,[3] Jessica Campos-Delgado,[4] José Manuel Romo-Herrera,[4] Hyungbin Son,[2] Ya-Ping Hsieh,[2] Alfonso Reina,[1] Jing Kong,[2] Mauricio Terrones,[4] Mildred S. Dresselhaus[2,5]*

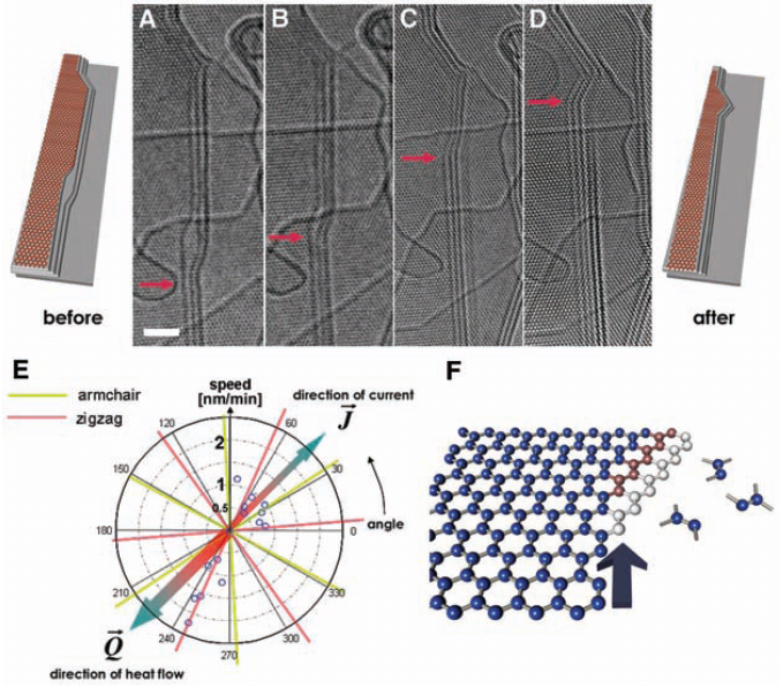

Dai Lab,
Nature Phys. **7**, 616 (2011)

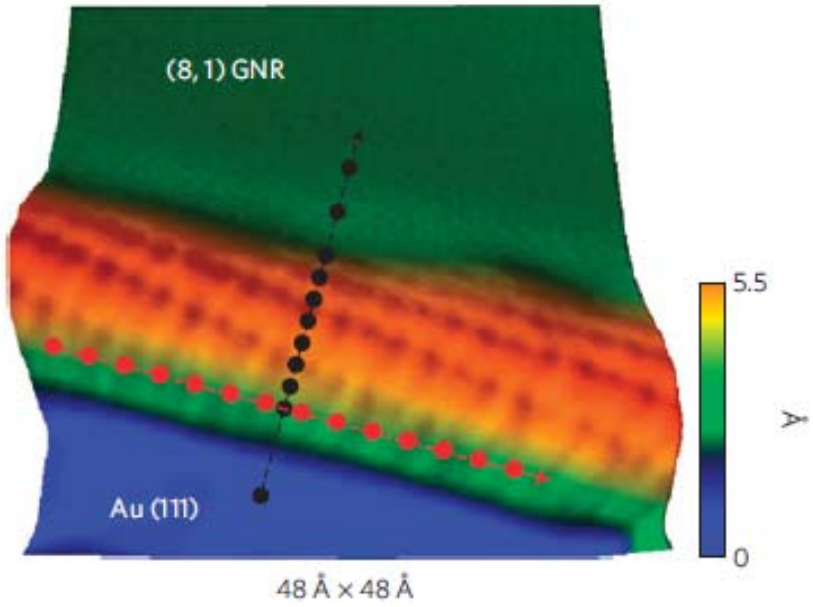

Thermoelectricity in Single-Molecule Nanojunctions (see mini-review arXiv:1111.0106)

Majumdar Lab, Science **315**, 2568 (2007)

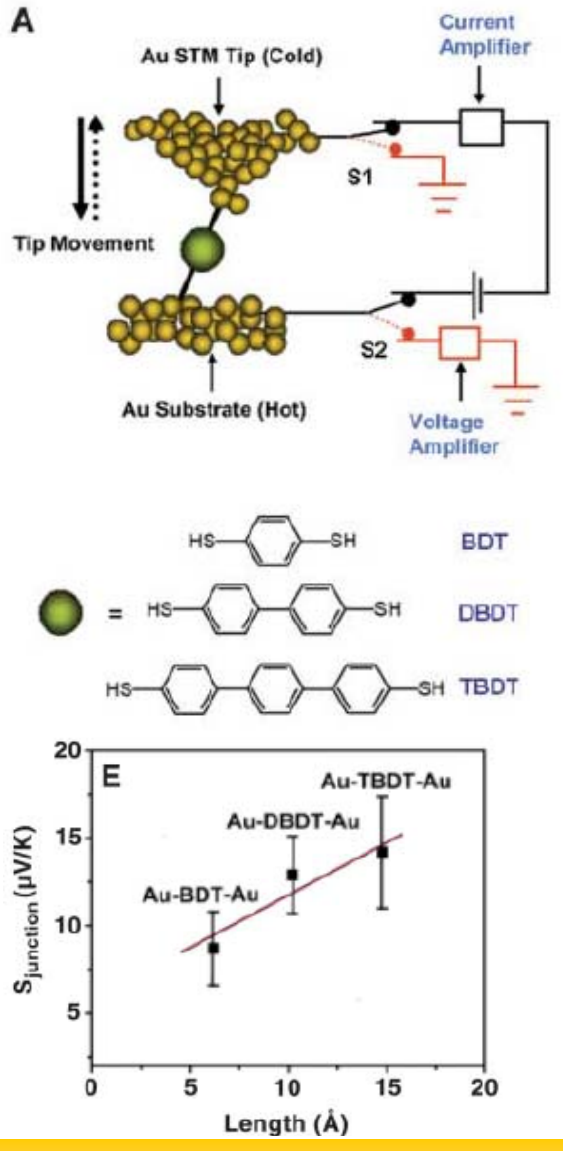

Cuniberti group, PRB **81**, 235406 (2010)

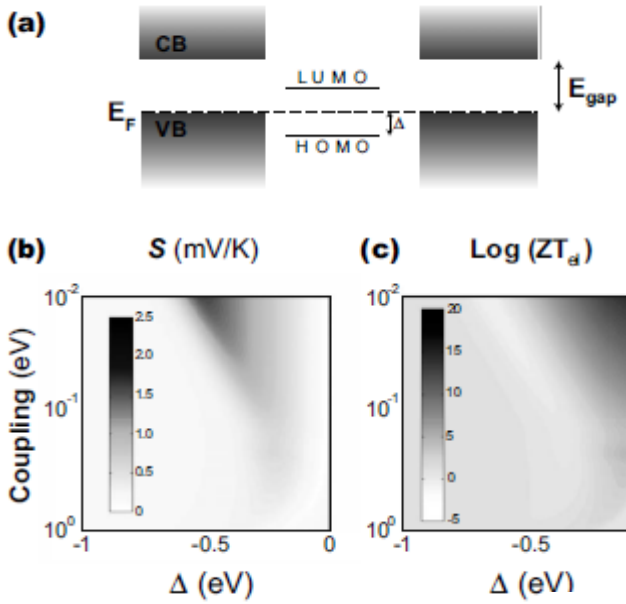

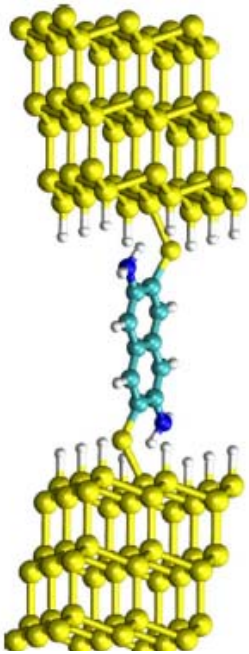

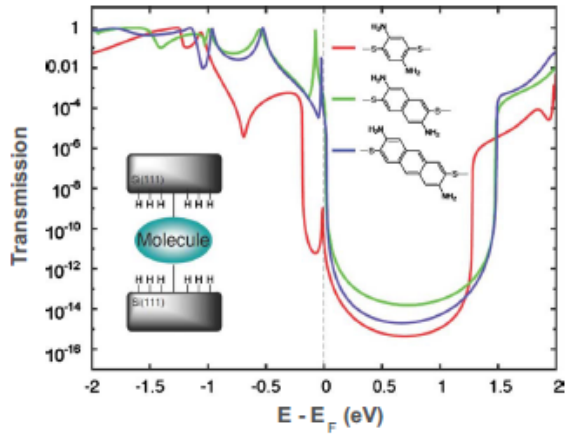

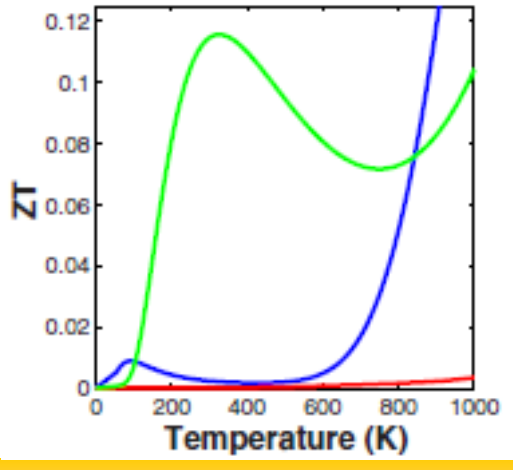

Toward Metal-Free Molecular Electronics

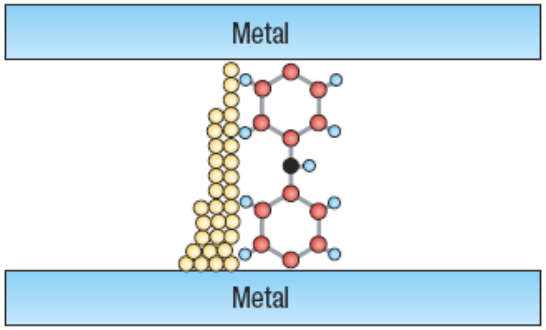

❑Control of the contact structure between an organic molecule and a metal electrode (usually gold) is difficult because bonding to metal atoms, although potentially strong, **is not strongly directional**, leading to **poor reproducibility** of most metal-molecule-metal junctions.

Nature. Mater. **5**, 63 (2006)

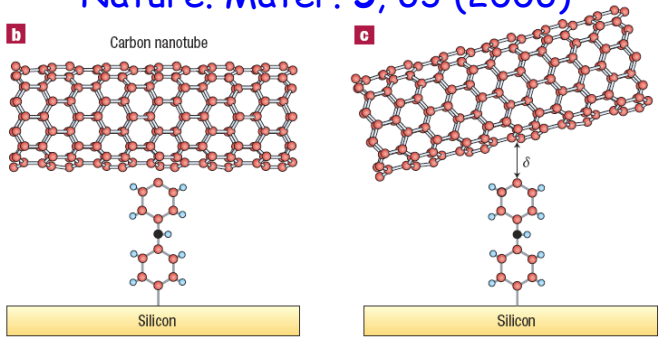

Science **311**, 356 - 359 (2006)

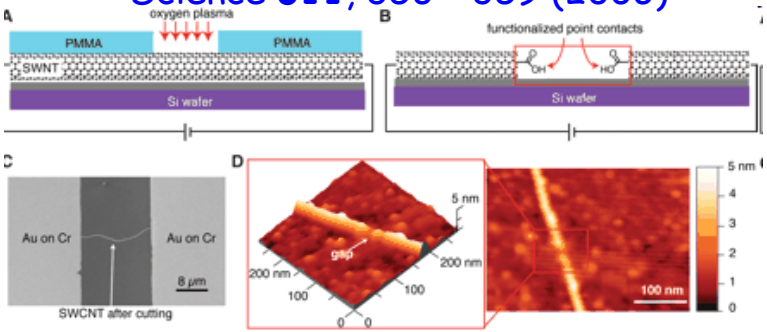

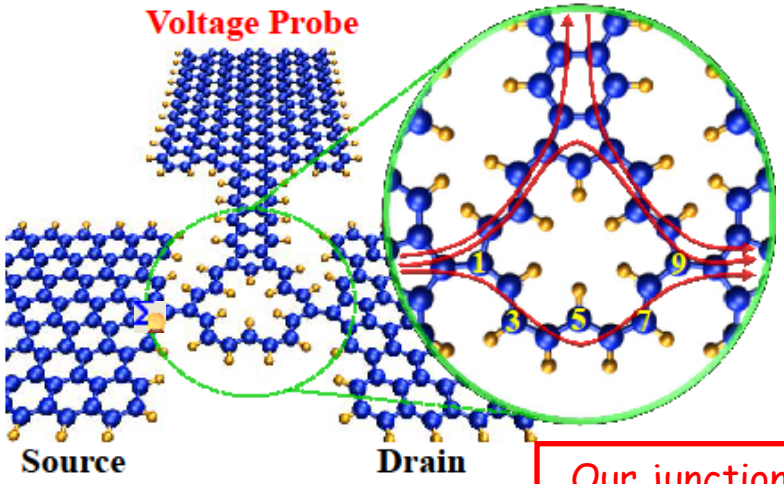

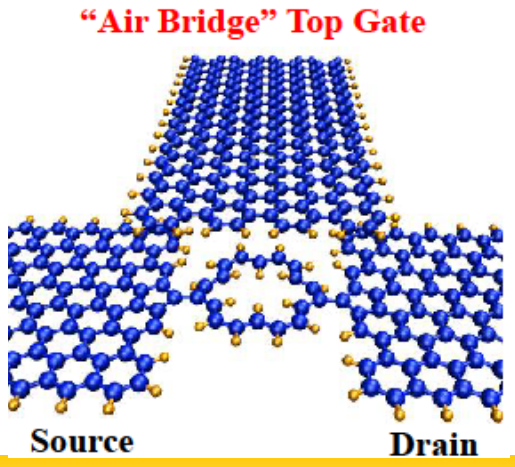

Our junctions with strong molecule-electrode coupling evade problems due to the lack of **derivative discontinuity** in continuous local and semi-local DFT approximations (LDA and GGA) as a **major source of error** in calculating the *I-V* characteristics

Nikolić group, PRL **100**, 236803 (2010)

ZGNR|molecule|ZGNR Thermoelectric Devices Based on Evanescent Mode Transport

ZGNR|18-annulene|ZGNR

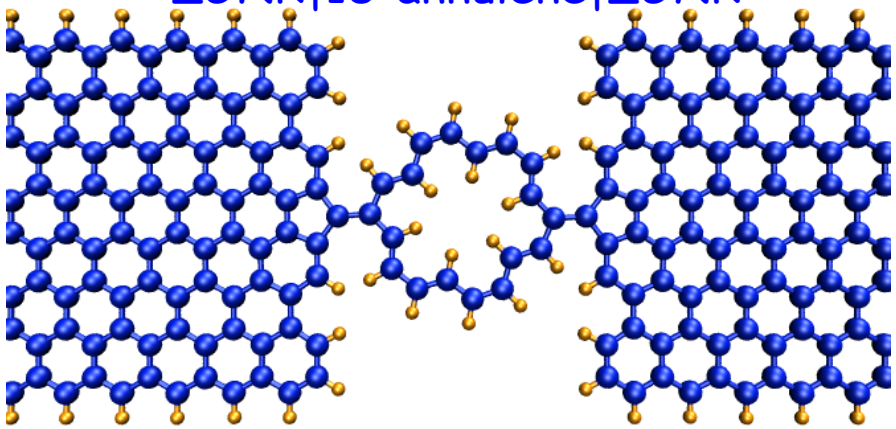

Nikolić group, PRB **84**, 041412(R) (2011)
+ J. Comp. Electronics **11**, 78 (2012)

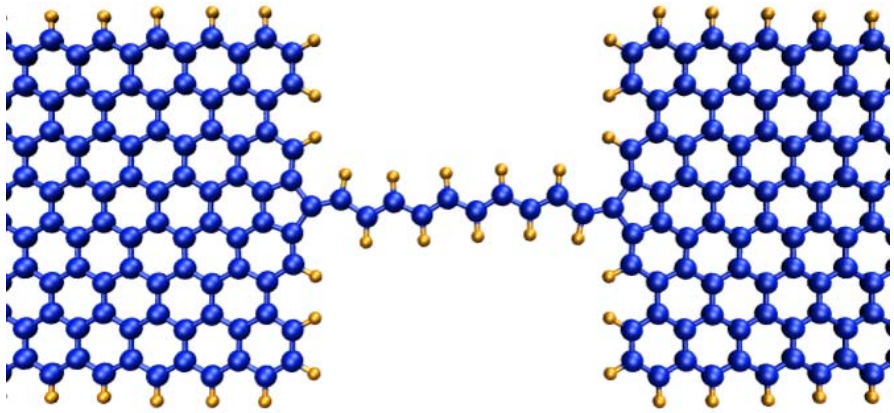

ZGNR|C10|ZGNR

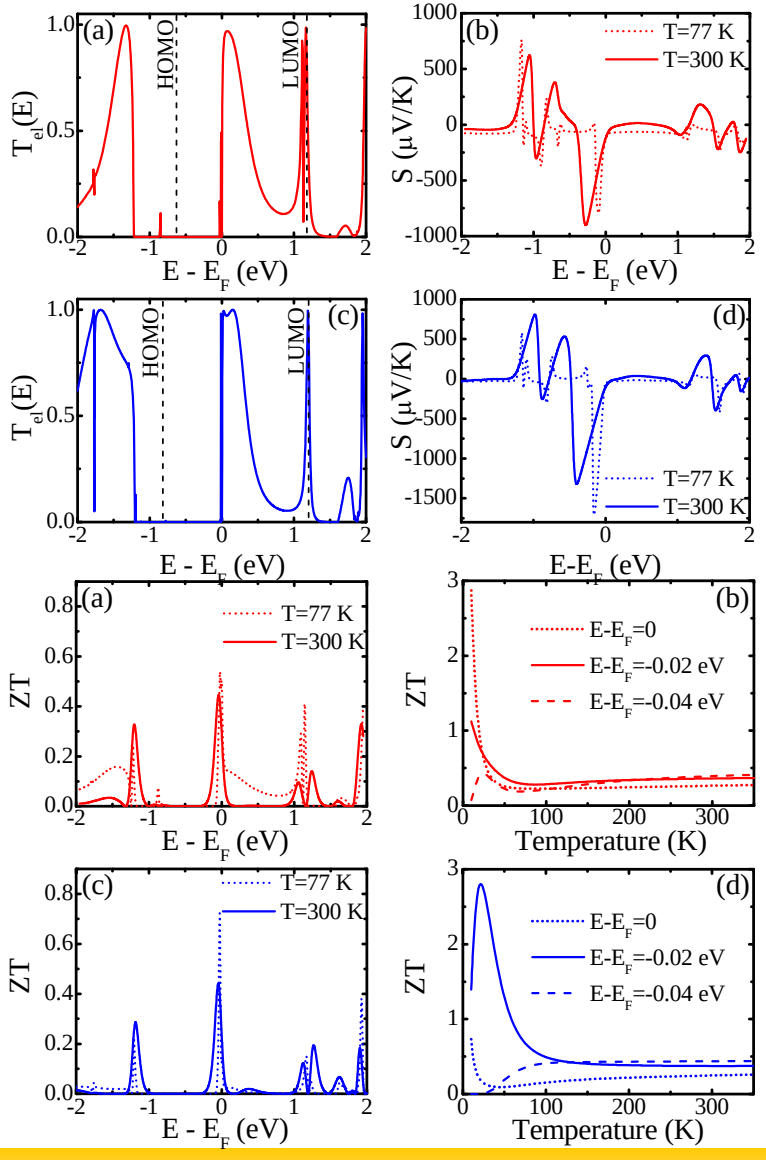

Three-Terminal Single-Molecule Nanojunction Thermoelectrics

Nikolić group, PRB **84**, 041412(R) (2011)

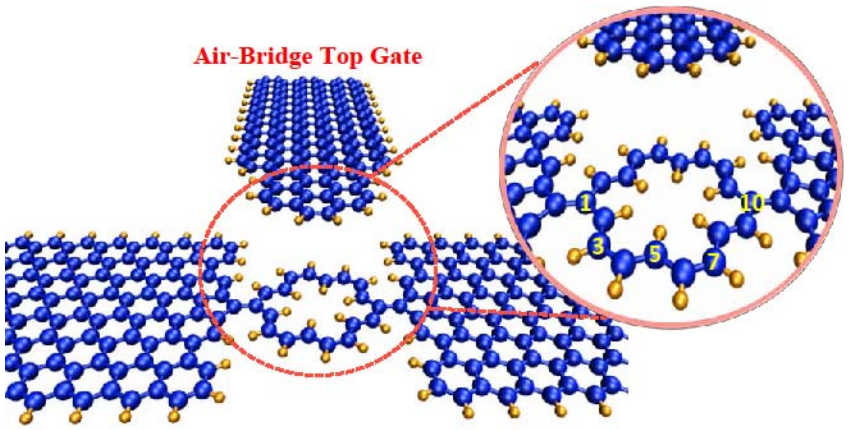

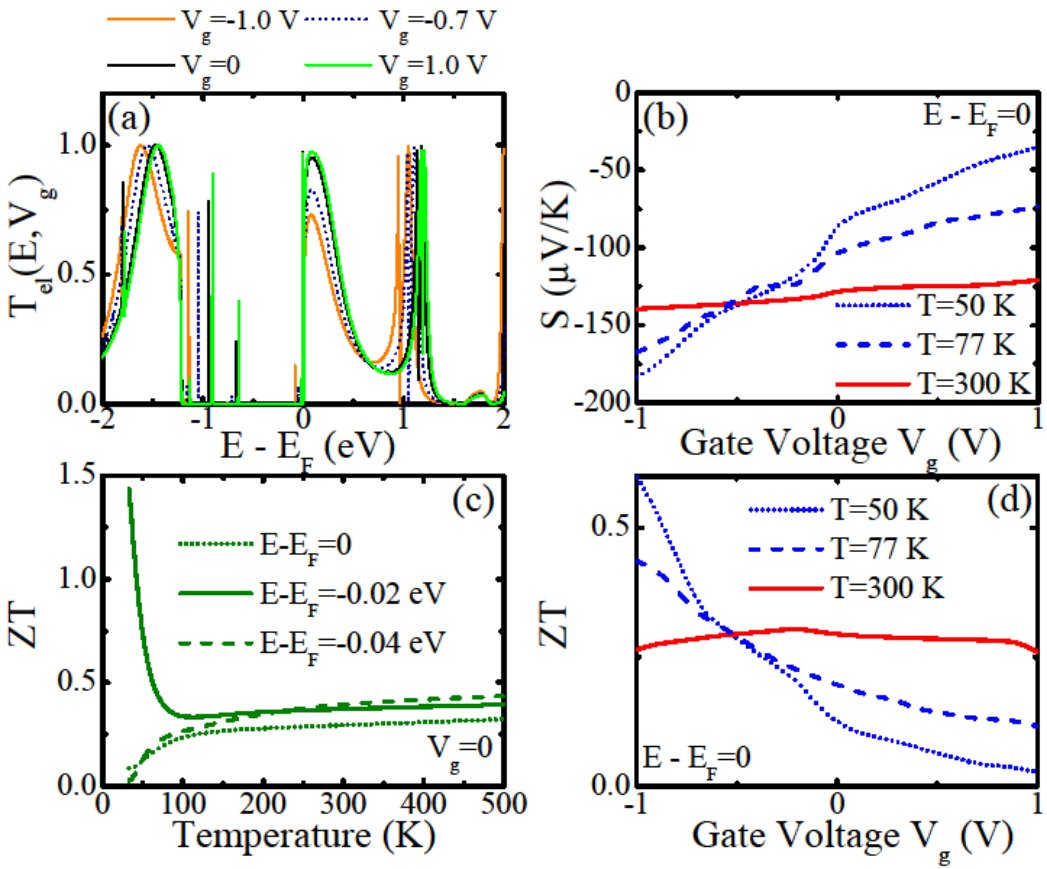

Fabrication of Single-Molecule Nanojunctions with Graphene Electrodes

van der Zant Lab, Nano Lett. **11**, 4607 (2011)

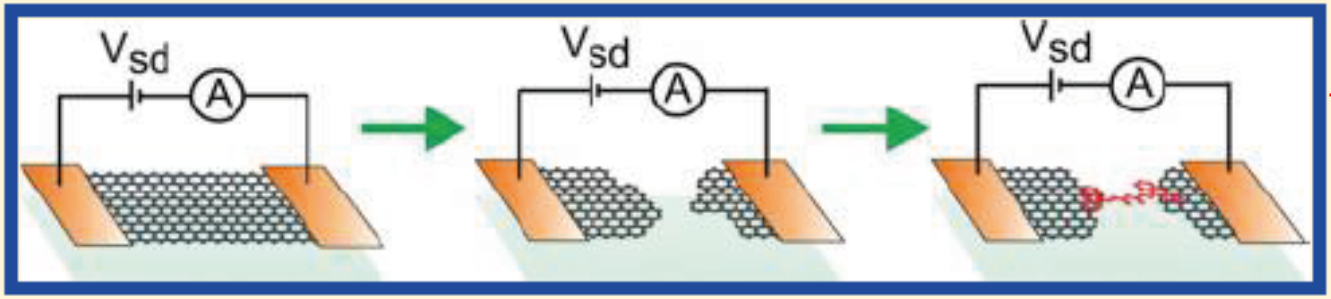

depositing molecules inside a few-layer graphene nanogap (of the size 1-2 nm) formed by feedback controlled electroburning

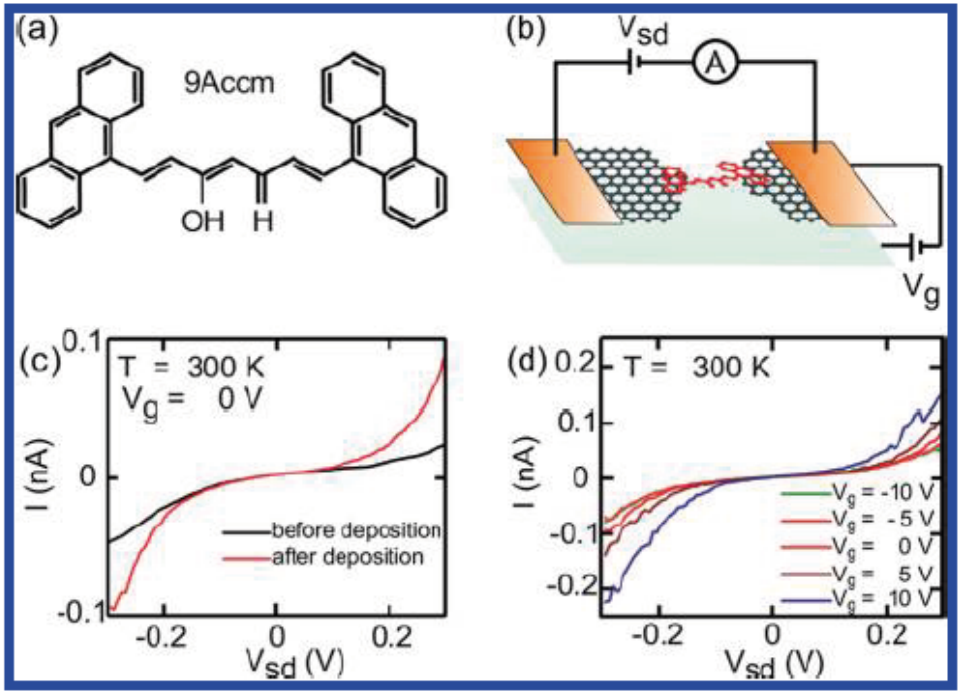

Gatable I-V characteristics at room temperature

Conclusions in Pictures

Empirical versus first-principles phonon transport modeling:

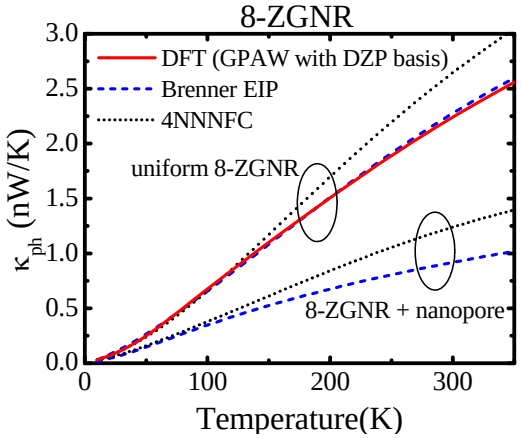

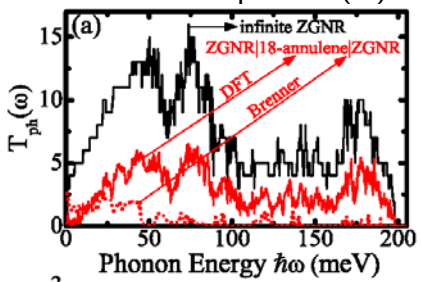

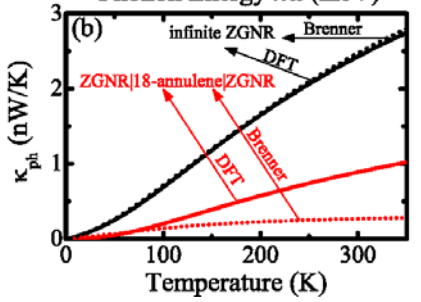

Edge currents and nanopores in GNR thermoelectrics:

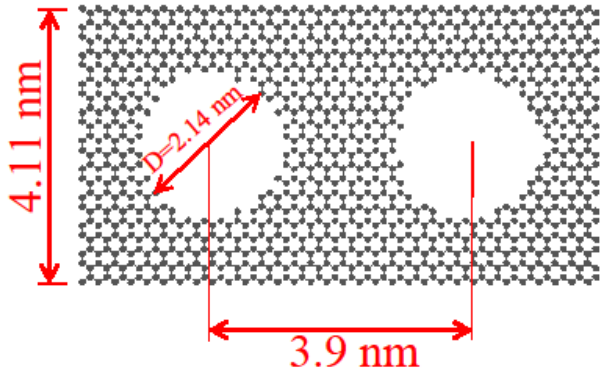

Evanescent mode transport in single-molecule nanojunctions to optimize power factor: